# Metadata of the article that will be visualized online

| | | |
|---|---|---|
| ArticleTitle | | Probabilistic landslide hazard assessments: adaptation of spatial models to large slow-moving earth flows and preliminary evaluation in Loja (Ecuador) |
| Article CopyRight - Year | | The Author(s), under exclusive licence to Springer-Verlag GmbH Germany, part of Springer Nature 2024 |
| Corresponding Author | Family Name | Galve |
| | Particle | |
| | Given Name | Jorge P. |
| | Organization | Universidad de Granada |
| | Address | Campus Fuentenueva s/n Granada 18071, Spain |
| | Division | Departamento de Geodinámica, Facultad de Ciencias |
| | Email | jpgalve@ugr.es |
| Author | Family Name | Luzuriaga |
| | Particle | |
| | Given Name | John Soto |
| | Organization | Universidad Técnica Particular de Loja |
| | Address | Loja AP 1101608, Ecuador |
| | Division | Departamento de Geociencias |
| Author | Family Name | Palenzuela |
| | Particle | |
| | Given Name | José Antonio |
| | Organization | ETSICCP, University of Granada |
| | Address | Campus Fuentenueva s/n Granada 18071, Spain |
| | Division | Department of Civil Engineering |
| Author | Family Name | Azañón |
| | Particle | |
| | Given Name | José Miguel |
| | Organization | Universidad de Granada |
| | Address | Campus Fuentenueva s/n Granada 18071, Spain |
| | Division | Departamento de Geodinámica, Facultad de Ciencias |
| Author | Family Name | Tamay |
| | Particle | |
| | Given Name | José |
| | Organization | Universidad Técnica Particular de Loja |
| | Address | Loja AP 1101608, Ecuador |

| | | |
|---|---|---|
| | Division | Departamento de Geociencias |
| Author | Family Name | Jaramillo |
| | Particle | |
| | Given Name | Galo Guamán |
| | Organization | Universidad Técnica Particular de Loja |
| | Address | Loja AP 1101608, Ecuador |
| | Division | Departamento de Geociencias |
| Author | Family Name | Irigaray |
| | Particle | |
| | Given Name | Clemente |
| | Organization | ETSICCP, University of Granada |
| | Address | Campus Fuentenueva s/n Granada 18071, Spain |
| | Division | Department of Civil Engineering |
| | | |
|---|---|---|
| Schedule | Received | 1 May 2024 |
| | Revised | |
| | Accepted | 3 October 2024 |

Abstract

Quantitative landslide hazard models provide estimations of the number of landslides per area and time that might be expected in the near future. These models are essential to calculate landslide risk in monetary terms. Although they are very useful tools for managing the activity of unstable slopes, their production calls for a vast amount of spatial and temporal data. Here, we present a case where this was possible producing the quantitative landslide hazard map for the municipality of Loja, Ecuador. It is based on a model that integrates six causal factors (distance to faults, lithology, slope, geomorphology, topographic position index, land use) and a comprehensive multi-temporal inventory of landslides. First, a susceptibility map was generated with a good prediction capability (Area under prediction rate curve, AUPRC: 0.8) combining two widely used and tested probabilistic methods: “Matrix” and “Likelihood ratio”. Subsequently, this map was transformed into a hazard map by including the temporal frequency of landslides. The map assesses the annual probability of each pixel to be set in motion within one of these landslides. The preliminary temporal validation of the hazard map indicates that the pixels mobilized during two years after the map production fit reasonably well with our spatio-temporal forecast. The findings emphasize that classical spatial prediction methods, when augmented by robust and extensive data on landslide distribution and activity, can yield hazard models with reliable predictive capabilities. This suggests that in practical applications, models based on relatively simple calculations can provide effective and reliable starting points for managing landslide risks.

Keywords(seperated by –)

Matrix–
Likelihood ratio–
Multitemporal inventories–
Prediction models–
Cross-validation–

Environmental Earth Sciences _####################_
https://doi.org/10.1007/s12665-024-11905-7

ORIGINAL ARTICLE

# Probabilistic landslide hazard assessments: adaptation of spatial models to large slow-moving earth flows and preliminary evaluation in Loja (Ecuador)

John Soto Luzuriaga[1] · Jorge P. Galve[2] · José Antonio Palenzuela[3] · José Miguel Azañón[2] · José Tamay[1] · Galo Guamán Jaramillo[1] · Clemente Irigaray[3]

Received: 1 May 2024 / Accepted: 3 October 2024


## Abstract

Quantitative landslide hazard models provide estimations of the number of landslides per area and time that might be expected in the near future. These models are essential to calculate landslide risk in monetary terms. Although they are very useful tools for managing the activity of unstable slopes, their production calls for a vast amount of spatial and temporal data. Here, we present a case where this was possible producing the quantitative landslide hazard map for the municipality of Loja, Ecuador. It is based on a model that integrates six causal factors (distance to faults, lithology, slope, geomorphology, topographic position index, land use) and a comprehensive multi-temporal inventory of landslides. First, a susceptibility map was generated with a good prediction capability (Area under prediction rate curve, AUPRC: 0.8) combining two widely used and tested probabilistic methods: "Matrix" and "Likelihood ratio". Subsequently, this map was transformed into a hazard map by including the temporal frequency of landslides. The map assesses the annual probability of each pixel to be set in motion within one of these landslides. The preliminary temporal validation of the hazard map indicates that the pixels mobilized during two years after the map production fit reasonably well with our spatio-temporal forecast. The findings emphasize that classical spatial prediction methods, when augmented by robust and extensive data on landslide distribution and activity, can yield hazard models with reliable predictive capabilities. This suggests that in practical applications, models based on relatively simple calculations can provide effective and reliable starting points for managing landslide risks.

**Keywords** Matrix · Likelihood ratio · Multitemporal inventories · Prediction models · Cross-validation

## Introduction

Landslides are currently one of the natural disasters of most frequent reoccurrence. Other phenomena, such as earthquakes, take place less frequently and in fewer places worldwide. The destructive potential of landslides, in terms of human and monetary losses, increases when there is urban development nearby (Aleotti and Chowdhury 1999; Guzzetti et al. 1999). Thus, the damage derived from landslides is more severe when urban growth sprawls over gemorphologically and geologically critical zones having high slopes and elevations, unfavourable lithology, discontinuities, and other specific geological features. In some cases, critical areas are affected by land use and anthropic actions that favour the development of mass movements. This fact is well documented in the literature related to landslides (e.g., Unesco 1973-79; Arnould and Frey 1977; Schuster and Krizek 1978; Aleotti and Chowdhury 1999; Guzzetti et al. 1999; Irigaray et al. 2000; Cardinali et al. 2002; McBean and Henstra 2003; Haque and Burton 2005; O'Hare and Rivas 2005; Petley et al. 2005; Larsen 2008;

✉ Jorge P. Galve
jpgalve@ugr.es

[1] Departamento de Geociencias, Universidad Técnica Particular de Loja, Loja, AP 1101608, Ecuador

[2] Departamento de Geodinámica, Facultad de Ciencias, Universidad de Granada, Campus Fuentenueva s/n, Granada 18071, Spain

[3] Department of Civil Engineering, ETSICCP, University of Granada, Campus Fuentenueva s/n, Granada 18071, Spain

Lacasse and Nadim 2009; Petley 2012; Palenzuela et al. 2016; Soto et al. 2017; Girma et al. 2015; Raghuvanshi et al. 2015; Hamza 2017).

Countries are struggling to cover the costs of landslide-related damage or slope stabilization measures. In the period between 2004 and 2010, a total of 2,620 fatal landslides were recorded worldwide, causing 32,322 deaths (Petley 2012; Palenzuela 2015). In China, 15,403 landslides occurred in mountainous and non-mountainous regions during the year 2013, leading to 669 deaths or people who disapeared, as well as 264 injured, and a direct economic loss of 10.2 billion CNY (Chinese yuans) (Chen et al. 2016a). In the United States, urban landslides cause up to 25–50 deaths per year and some $ 3.5 billion in damage (Bowman 2015; Pollock 2020). In the Andean region, landslides are one of the greatest natural threats (Alcántara-Ayala and Oliver-Smith 2014; Petley 2012; Hermanns et al. 2012), entailing losses of millions of dollars and thousands of deaths. AQ1

In the case of Ecuador, of all the natural hazards, landslides cause the most widespread impact. Between 1970 and 2013, 3113 landslides were recorded in this country, mainly during the wettest months: January, February, March and April (Eras 2014). Other reports indicate that during the period 1970–2010, 19% of the 5,523 events associated with different natural hazards in Ecuador were landslides, and this type of phenomenon caused the highest number of victims and economic losses (SNGR / ECHO / UNIDR, 2012).

This global situation accentuates the need for a prevention strategy supported by hazard and risk models, early warning systems, and land-use planning. These are the most appropriate ways to minimize the human and economic losses caused by hillside movements (Aleotti and Chowdhury 1999; Chacón et al. 2006; Adedeji et al. 2012; dos Santos Alvalá et al. 2019). Hazard models involve estimating the probability of landslides occurring within a given area and time period, enabling correct management and planning to avoid or mitigate potential damage (Fell et al. 2008). For this purpose, data must be collected on the location and frequency of landslides (temporary inventories) or their triggers (mainly rain and seismicity) so as to generate hazard maps that would enable disaster prevention and correct land-use planning.

Currently, Geographic Information Systems (GIS) facilitate landslide analysis. By using a series of variables and large amounts of data to generate landslide predictive maps over large geographic areas, in a quick and efficient manner, these maps have been produced in diverse geological, climatic and socio-economical settings (e.g., Palamakumbure et al. 2015; Manchar et al. 2018; Nsengiyumva et al. 2019; Phong et al. 2021; Gantimurova et al. 2021). However, the extraordinarily wide range of landslide typologies, causal factors and methods makes it difficult to define a single methodology for the analysis and assessment of landslide hazard (Guzzetti 2002). There are several standard procedures for generating hazard maps on a detailed scale and different approaches may be adopted in view of the needs, data availability or objectives of each assessment (e.g. Fabbri et al. 2003; Corominas et al. 2003; Remondo et al. 2005; Fell et al. 2005; Bonachea 2006; Corominas and Moya, 2008; Corominas et al. 2014). The reliability of hazard maps depends significantly on the scale of the work, the quantity and quality of the data acquired, and the selection of the appropriate modelling methodology (Baeza and Corominas 2001; Pourghasemi et al. 2012; Chen et al. 2016b).

Among the many techniques already developed at the regional scale for modelling the landslide occurrence, there are statistical/probabilistical methods and Machine/Deep Learning algorithms. However, these techniques are generally applied for the assessment of landslide susceptibility, which only indicates the areas most prone to landslide, without specifying exactly when the landslides will occur in the future (van Westen et al. 2008; Fell et al. 2008). Even the most advanced methods, despite their complexity and robustness, do not necessarily enhance the forecasting capacity for future landslide prediction, as this capacity also depends on the quality of data inputs and the understanding of the applied method. From the review of Reichenbach et al. (2018) it can be concluded that nowadays it is more important to know how methods operate than to use a priori more powerful techniques without experience. Additionally, the quality of the input data for data-driven methods can prove more important than the technique used to produce a model.

Recently, some scholars are trying to include dynamic variables (such as triggering rainfall) as input for Machine Learning algorithms in order to create spatiotemporal forecasting models for landslides (Stanley et al. 2021; Li et al. 2022; Mondini et al. 2023; Fang et al. 2024; Moreno et al. 2024; Nocentini et al. 2024; Dahal et al. 2024).

In this paper, we describe the comprehensive production of multi-temporal landslide inventories as the basis for a complete landslide hazard assessment. In our case study, a landslide hazard model of the city of Loja (Ecuador) is produced using all the information compiled in the city over the past ten years. Two classical approaches are used to initially estimate landslide susceptibility. We needed to adapt these approaches to accommodate our object of study: large slow-moving earth flows—a type of landslide that does not align well with analyses designed for predicting new slope instabilities, such as rainfall-induced shallow landslides. For shallow landslides, each pixel or small group of pixels or spatial units typically corresponds to a single occurrence and an area where variables do not change significantly, while large landslides often span numerous pixels

involving diverse conditions in the variables. Additionally, unlike shallow landslides, which are short-lived and quickly eroded after a single event, earth flows persist in the landscape and can be reactivated by future heavy rains. This aspect also complicates the analysis that commonly relies on a simple absence/presence (0/1) binary system. Predictive models are generally designed to forecast where new landslides might occur—essentially where the absence of a process turns into its presence, as with shallow landslides. However, when input data include large portions of terrain that has already slid and may do so repeatedly, the methods used to generate susceptibility and hazard models struggle to model these cases. The straightforward binary approach becomes more complex and loses its pure boolean nature, transforming into a slightly more complicated scenario. Thus, our objective is to develop a thorough landslide hazard study of large slow-moving earth flows overcoming the problems explained above, to serve as an example for similar studies. Our first innovation is a change in the purpose of the models: not just to indicate currently stable terrain that will slide in the future (as in typical rainfall-induced shallow slide susceptibility models), but also to indicate landslide terrain that is prone to reactivate its movement in the next rainy season (see, e.g., Soto et al. 2017). Our second innovation is an evaluation of the forecasting capability of the hazard model. Although preliminary, it is the first of its kind within the specialized literature.

## Study area

The study area is located in southern Ecuador and covers the city of Loja (Fig. 1). Geologically speaking, this city was built over an intra-montane sedimentary basin of the same name. The Loja Basin is one of several Neogene intramontane basins described in southern Ecuador (Fig. 1a). Its lacustrine origin is traced to Miocene-Pliocene times (Hungerbühler et al. 2002). The sequence, from bottom to top, comprises: (1) coarse-grained sandstones with thin layers of conglomerate, sand and mudstones of the Trigal Formation; (2) limestones, thin layers of carbonate mudstones, layers of chert (silica), and yellow sandstones of the La Banda Formation; (3) layers of sandstones intercalated with conglomerates of the Belen Formation; (4) sandstones, carbonaceous and siliceous mudstones, diatomites, lignites, and conglomerate intercalations of the San Cayetano Formation; (5) conglomerates of the Quillollaco Formation; and (6) heavily weathered lithic tuffs of the Salapa Formation of pyroclastic origin (volcanic). The above sedimentary sequence fills a Paleozoic metamorphic basement made up of impure fine to medium grain quartzites, black phyllites, slates and schists (Hungerbühler et al. 2002) (Fig. 1b). According to Tamay et al. (2016), structurally, the Loja basin is characterized by having a reverse fault on the eastern edge with a NW-SE strike and vergence east, which has a greater deformation that is evidenced by the presence of folds. While, in the western edge it is characterized by having normal faults with dipping to the east (Fig. 1c).

According to Soto et al. (2017), the San Cayetano, Belén and Trigal formations show a high clay content of the smectite group. These minerals confer very high plasticity to the materials and contribute to the ground instability observed in Loja. The expansive behaviour of these clays, enhanced by the tropical climate, allows for low gradient slopes (10–15°) that can also favour ground sliding. This characteristic makes large sections of the Loja Valley susceptible to landslides.

The landscape of the Loja Valley is controlled by sloping and folded layers of the backfill, with a wide valley floor surronded by a hilly relief dominated by steep slopes. This rugged terrain is partially covered by the ninth largest city in Ecuador, Loja (170,280 inhabitants, INEC 2010). The urban expansion of this city in recent decades has taken place outside the area with the most stable terrain, invading the hill slopes at the bottom of the valley. In many cases, urban developers have underestimated the instability problems of these hillsides, and various slope movements have affected new neighbours, causing extensive damage and even fatalities (Soto et al. 2017). Loja could serve as an analogue for other cities in Ecuador and the northern Andes with similar problems related to unstable slopes.

Loja has humid subtropical conditions because of its latitude and elevation. The average annual rainfall is 917 mm, and the average monthly temperature is 16.2 °C. The period with the lowest average temperature lasts from June to September, July being the coldest month (14.9 °C) (PNUMA 2007; Soto et al. 2017). The most intense rainfall is concentrated in the period from December to April, the humid season, but precipitation continues throughout the year.

The study area acts as a natural laboratory to test the proposed procedure. Most of the geological parameters related to unstable slopes are well constrained by previous detailed research work (see Tamay 2018; Soto et al. 2017, 2019; Soto 2018 and references therein). Furthermore, because the analyzed earth flows are very active in the region, a wealth of data on their activity can be obtained in a few years. The area therefore affords ideal conditions to develop landslide hazard models and subsequently validate them.

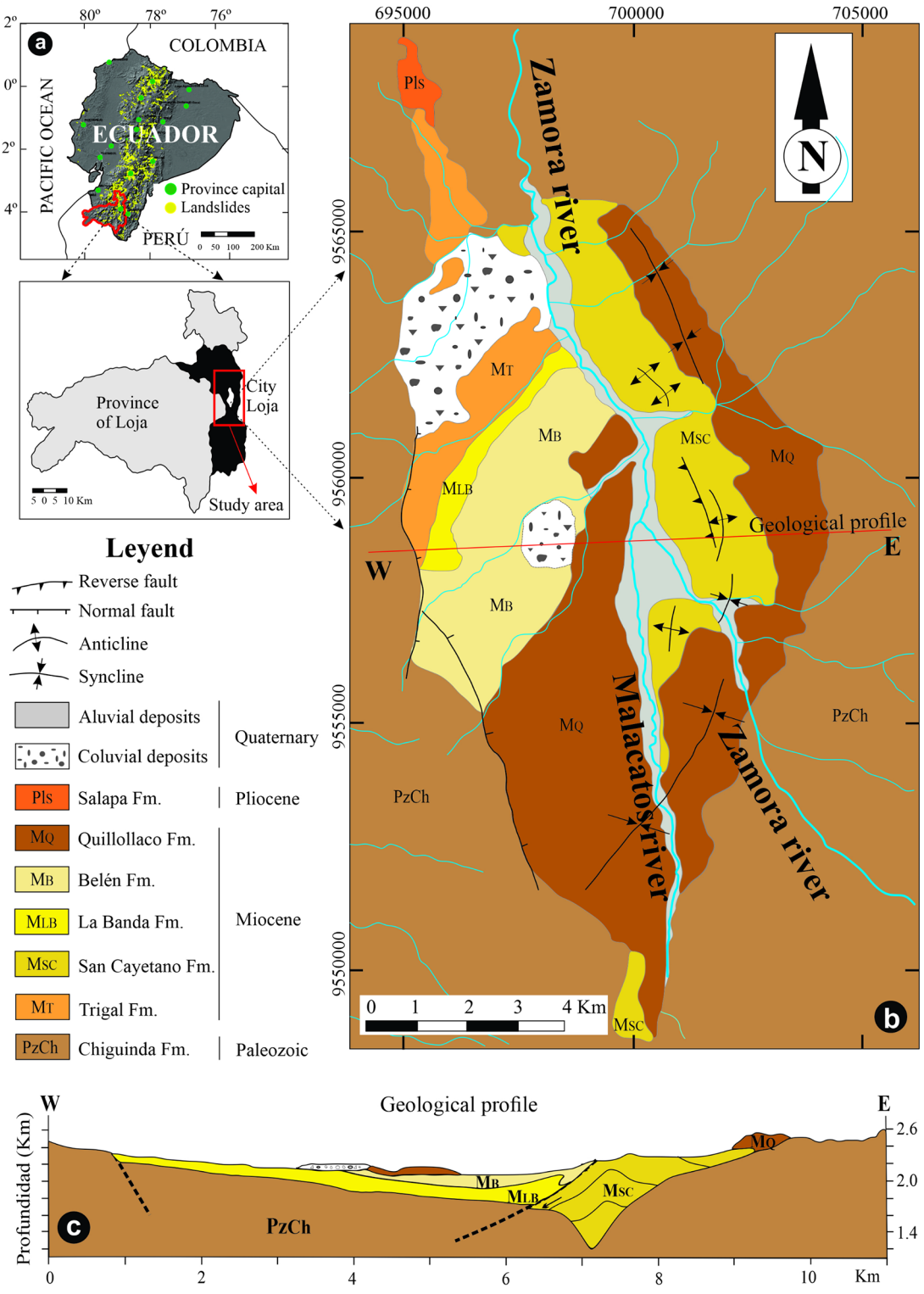


**Fig. 1** Location sketch of the studied area (**a**) with respect to Ecuador (**b**) simplified geological map (**c**) geological cross section. (b and c, modified of Tamay et al. 2016)

## Methodology

We applied a metrodology comprising two main steps: (1) analysis of the spatial landsliding potential (susceptibility), and (2) estimation of the spatio-temporal probability of landsliding (hazard). The hazard models presented here are based on an analysis of the spatio-temporal distribution of landslides over the last two decades, using statistical techniques. This period was chosen because there is no information available on landslides prior to 1999. A detailed inventory of landslides was carried out in the study area over a period of 16 years (1999–2015), considering the spatial and temporal distribution. The analysis is applicable for large landslides of a flow-type, as the general inventory shows a large percentage of landslides related to the type of creeping and flows (95%), generally involving creeping processes that later evolve into composite flows.

In this research, two statistical-probabilistic methods were applied and compared for the initial susceptibility assessment. Figure 2 indicates the work-flow procedure followed. The "Matrix" method (Irigaray 1995) was positively validated in the surroundings of the Cordillera Bética (Irigaray 1995; Fernández et al. 2000; Irigaray et al. 2007), while the "Likelihood Ratio" method (Chung and Fabbri 1999; Chung and Fabbri 2005; Chung 2006) has been successfully applied in various Earth Science fields, and specifically to landslides (e.g., Remondo et al. 2003; Zêzere et al. 2004; Lee and Talib 2005; Chung and Fabbri 2008; Carrara et al. 2008; Galve et al. 2015). Although these may be considered as classical methods, they have proven to perform well and are still used nowadays in landslide research (e.g., Boualla et al. 2019; Barella et al. 2019; Kavoura and Sabatakakis 2020; Gerzsenyi and Albert 2021; Sahrane et al. 2022). Furthermore, these techniques allow easily to measure the participation of each variable in the prediction model which allows actions to be taken on improving the most predictive variables to increase the forecasting capability of the models (see e.g., Lee and Talib 2005 and Galve et al. 2009,

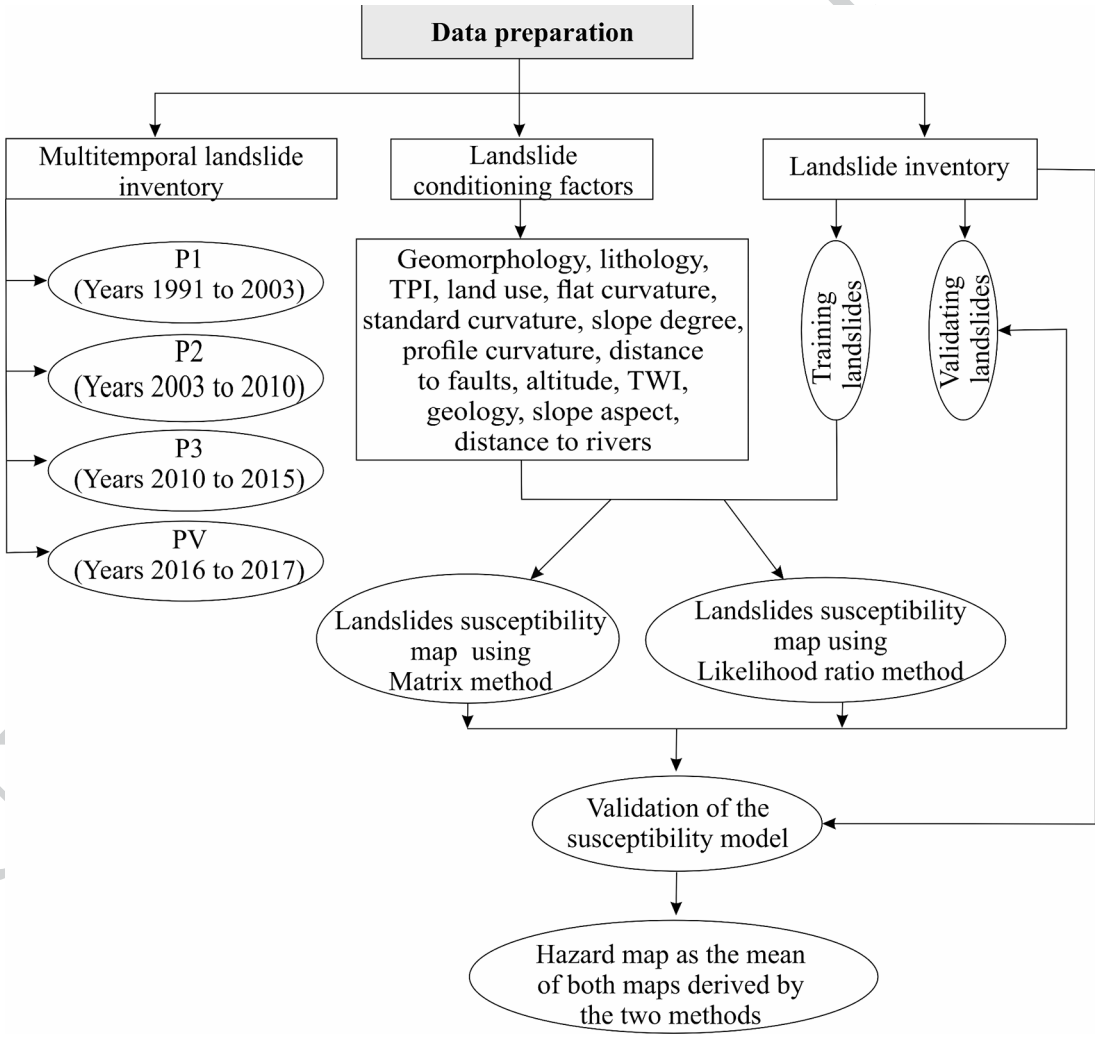


**Fig. 2** Flowchart of the methodology used

2015). We applied them because they can be applied using the tools included in most common GIS softwares. Thus, these methods can be implemented by many technicians who may not have specialized expertise in predictive models, such as those required for advanced machine learning and deep learning techniques.

## Landslide inventories and conditioning factor database

A fundamental and determining aspect for any assessment of susceptibility, hazard or landslide risk is the inventory and mapping of landslides occurrence, as key input determining the quality of the results. Therefore, the very first step is to collect information on past landslides, crucial for the prediction of future spatial distribution (Ercanoglu and Gokceoglu 2004). Among the most commonly used techniques are photointerpretation with stereoscopic vision, LiDAR DEM analysis and field work (Wieczorek & Glade 2005; Einstein 1988; Soeters and van Westen 1996; Palenzuela 2015). In this study, two techniques were used to carry out the landslide inventory. The first consists of applying photo interpretation to map slope movements with their respective field validation, and thus generate the inventory between 1999 and 2003 using aerial photographs at a scale of 1: 7,000 from the year 2003. This inventory, the first ever carried out in Loja province, coincided with the first time that an emergency caused by landslides was declared in Loja. For the inventory from 2003 to 2010, a 1:5,000 scale orthophoto of the year 2010 is used. Meanwhile, to generate the inventory for the period 2010 to 2015, field geomorphological mapping was applied exclusively, with a topographic map at a scale of 1:5,000 from a Digital Terrain Model (DTM) having a pixel resolution of 3 m (SIGTIERRAS 2010). All data was collected in a geodatabase generated with ArcGIS 10.1™, along with additional data corresponding to location, typology, degree of activity, lithology, terrain morphometry, date of occurrence, and derived damage.

Then, 14 raster maps representing landslide conditioning factors were created at 3 m of resolution (Fig. 3). Four of them consisted of field thematic cartography at a scale of 1:5,000, including: geomorphology, land use, lithology, geology and distance to faults (Table 1). Nine factors were extracted by processing the DTM: elevation, slope, aspect, flat curvature, standard curvature, profile curvature, distance to rivers, Topographic Wetness Index (TWI) (Seibert et al. 2007) and Topographic Position Index (TPI) (Persichillo et al. 2017).

Selection of the conditioning factors took into account the specialized literature on landslide susceptibility models (Feizizadeh and Blaschke 2013; Ozdemir and Altural 2013; Hamza and Raghuvanshi 2017; Reichenbach et al. 2018; Lima et al., 2022), but also the authors' experience in the study of behavioural characteristics of earth flows. The previous study by Soto et al. (2017) laid the foundations for the choice and treatment of geological data to derive lithology and geology factors. This research also appraised the geomorphic characteristics of the relief in terms of the occurrence of landslides. Thus, common factors related to slope geometry derived from DEMs —e.g., slope, curvature types and aspect— were also completed with a map of geomorphological units (i.e., the geomorphology factor) and the TPI factor. The "distance to rivers" factor was selected in view of fluvial erosion processes at the base of the slopes. The TWI factor was chosen because of the strong relationship between the reactivation of slope movements and surficial moisture conditions. Land use is an omnipresent factor in this type of analysis, while the "distance to faults" factor was selected because of possible increased fracturing of the bedrock as a function of its proximity to faults.

The continuous factors were reclassified according to the following procedures. Classification by intervals of the DEM were made for every 100 m of altitude, considered representative for the scale of work, except for the first interval (which ranges from the lower altitude of the study area, 1,979 to 2,000 m a.s.l.) and the last interval (from 2,600 to 2,642 m a.s.l., as the upper altitude of the study area). These ranges have been applied in the USA for slope movement susceptibility modelling (e.g., Highland and Bobrowsky 2008). Regarding the slope factor, we follow the classification used by Chen et al. (2018) or Van Westen (2016). The curvature, distance and TWI models were classified following our own expert criteria and knowledge of how these variables can affect earthflows.

## Susceptibility modeling

Susceptibility analysis was performed under a probabilistic approach, using spatial data analysis techniques, by means of the two methods described below.

### The "matrix" method

This method is a bivariate statistical quantitative procedure (DeGraff and Romesburg 1980; Irigaray 1995) to establish an instability index of a certain area. Although it cannot predict landslide susceptibility in terms of absolute probability, it allows one to evaluate the relative potential instability in a wide region by using a series of quantifiable values.

The "Matrix" method is founded on the generation of unique conditions units (UCUs), for which a landslide-susceptibility matrix (LSM) value is calculated. The UCUs are generated by overlapping the categorized maps of condition factors. The LSM value is the percentage of unstable

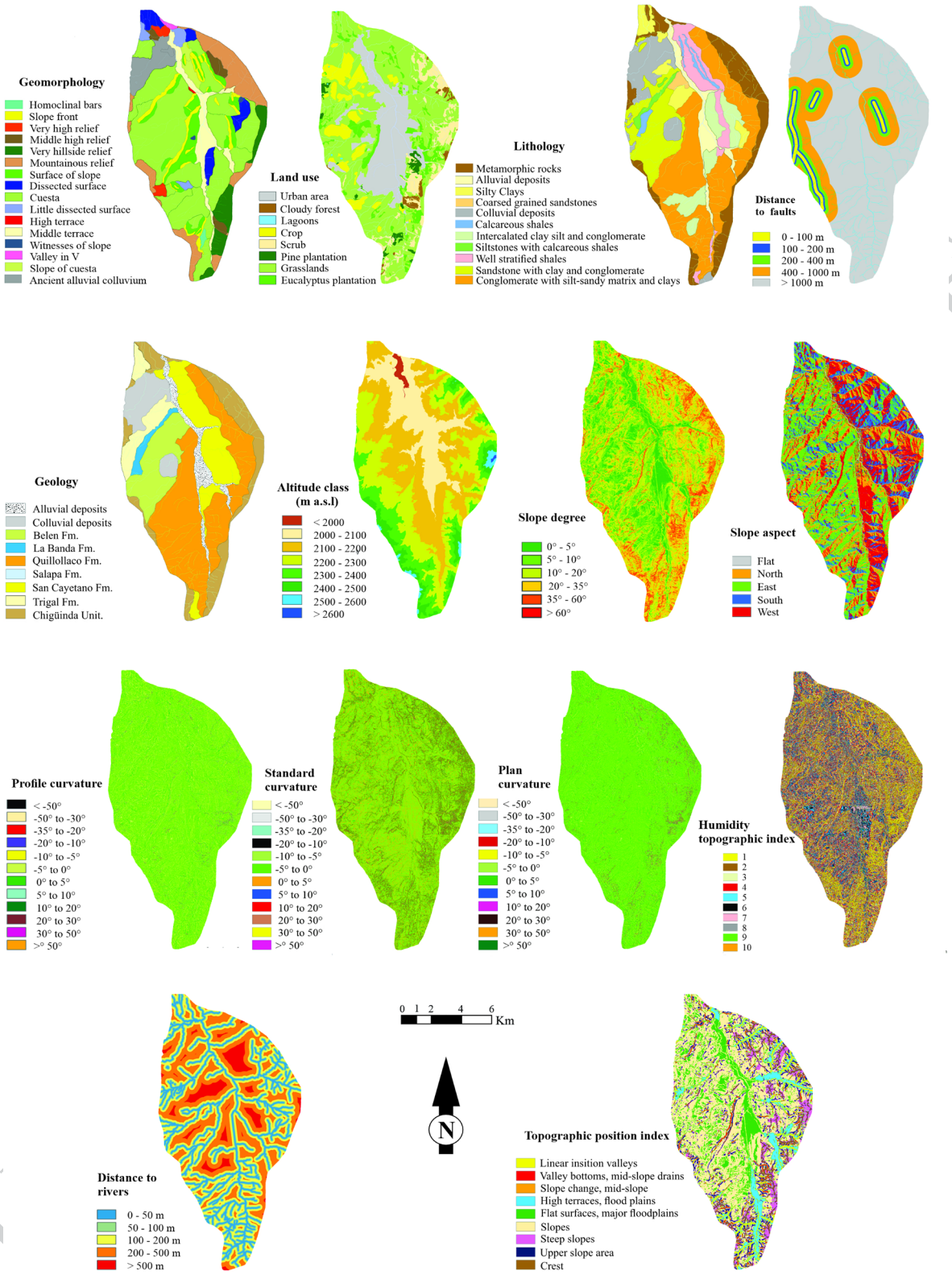


**Fig. 3** Thematic maps produced in this study

**Table 1** Causal factors, source and scale of maps

| Conditioning factors | Source | Scale |
|---|---|---|
| Geomorphology | Cueva 2015; Soto 2018. | 1:10,000 |
| Land use | Modified from Carrillo 2010; Orthophotos of the Loja basin (SIGTIERRAS 2010); Soto 2018. | 1:25,000 |
| Lithology | Soto 2010, 2018. | 1:25,000 |
| Geology and faults | Tamay et al. (2016). | 1:25,000 |
| Altitude, slope aspect, profile curvature, flat curvature, standard curvature, slope, Humidity Topographic Index, distance to rivers, topographic position index. | SIGTIERRAS 2010. Digital Terrain Model (DTM), with a pixel resolution of 3 m. | 1:5,000 |

area within the UCU. Once the LSM value is calculated for each UCU, the latter are sorted according to the LSM value, from the highest to the lowest; they are then assigned to five susceptibility classes following that order. The LSM range of these five classes can be determined using the natural-breaks method. A detailed explanation of the method can be found in Irigaray et al. (2007).

### The likelihood ratio (LR) method

This method is a probabilistic analysis based on favorability functions (Chung and Fabbri 1993). The LR method using categorical variables estimates the susceptibility by means of Eq. 1

$$LR_x = \frac{u_x/u}{s_x/s} \quad (1)$$

where $LR_x$ is the Likelihood Ratio estimated for the category $x$ of a variable; $u_x$ is the area occupied by unstable ground in the category $x$; $u$ is the total area covered by the unstable ground in the study area; $s_x$ is the area occupied by stable ground in the category $x$; and $s$ is the total area of stable terrain in the study area. In other words, $u_x/u$ is the proportion of unstable terrain within the area of the category $x$ and $s_x/s$ is the proportion of stable terrain within the same category $x$. If these proportions calculated for each category of a variable are different from one another, it means that the variable can explain the distribution of the unstable terrain, and therefore it has predictive capability.

By applying Eq. 1, each category of each variable has a LR value, and the variable maps are transformed into LR maps. These LR maps are multiplied to obtain the final susceptibility map. The method and its mathematical development are described in greater detail in Chung (2006).

To define the variables involved in the analysis, a preliminary study was carried out for each individual factor to create a one-variable model. Thus, the conditioning factors were ordered and selected according to their predictive capacity and potential to point out the most susceptible areas. Being only a pre-emption to order variables, it was performed applying just one of the methods, in this case, the LR method; but the procedure could also have been carried out using the "Matrix" method.

**Validation of conditioning factors and models** In this study, a temporal validation was used to evaluate the prediction capability of the susceptibility models. We split the landslide inventory in two sub-samples according to the date of the landslides. The training dataset, used to produce the models, is constituted by landslides registered before and during 2010; and the test dataset, used to validate the models, is composed of landslides that occurred after 2010.

To evaluate the conditioning variables and the models, Prediction-Rate Curves (PRC) were generated (Chung and Fabbri 1995; Chung and Fabbri 2003). These cumulative frequency curves express, quantitatively and graphically, the proportion of inventory landslides not used in the generation of the model (i.e., test sample), which are located in areas with a certain level of susceptibility. This method has been frequently applied to evaluate landslide susceptibility models (Fabbri and Chung 2008).

The Area Under the Prediction-Rate Curve (AUPRC) was used as an index to quantitatively assess the forecasting power of the model. However, the shape or geometry of the curve is even more useful, since it provides valuable information on how the different susceptibility classes behave. In general, the more asymptotic and closer the curve to the ordinate axis in its initial section, the better the model for discriminating the area of greatest susceptibility. Similarly, the earlier the curve reaches 100% of the landslides, the better the definition of the least susceptible (i.e., stable) zones, hence the safest area. In other words, the shape of the PRCs showed us where the best performance of the models is located. PRCs show if the model is better at predicting areas where landslides are concentrated (i.e., very high susceptibility area) but not so well the areas with less landslides, or it provides a prediction with a clear "stable" area but it does not recognize or delimitate well where the most susceptible regions are. An example of this is presented in the results

section when the shape of the PRCs of the models produced using LR and Matrix methods are compared.

## Landslide hazard modeling

Hazard models are forecasts of the spatio-temporal probability of future landslides. In order to generate hazard models, it is important to analyse triggering factors such as precipitation, seismic activity and anthropic activity. Soto et al. (2019) performed an analysis to estimate the empirical threshold of critical rain that causes landslides in the city of Loja, Ecuador, concluding that a clear correlation could not be established between the climatic frequencies and the major rain events that provoke landslides. However, given the high frequency of landslides, allowing for constant data collection, a multi-temporal analysis based on field inventories of different time intervals could be used in this research for hazard assessment and validation.

Few studies have addressed this problem with sufficiently representative time series (e.g., Van Steijn 1991; Corominas, 1992; Cendrero et al. 1994; González-Díez 1995; 1999; Remondo 2001; Bonachea et al. 2009). Remondo (2001) points out that when an area has a time series of landslides, the probability of occurrence can be estimated, and used to prepare hazard maps, if the environmental conditions are relatively homogeneous, as in our study area.

We opted to produce the landslide hazard model by combining the susceptibility models generated. After trying different combinations, the maximum, mode and average between the normalized values of the "Matrix" model and the "Likelihood Ratio" model were validated. Finally, the combination-based on the average offered a greater predictive capacity and was selected, as will be explained in Sect. 4.2.1.

To transform the susceptibility values into hazard values, a methodology proposed by Fabbri et al. (2003), Remondo et al. (2005) and Bonachea (2006) was adopted. The method works by minimizing deviations from the observed frequencies of new landslides within each susceptibility class, ensuring that the total of all susceptibility classes sums to 1 as a spatial probability. Next, using an adjustment function and the temporal frequency of landslides, an annual probability value $P$ was calculated for each unit using the following equation (Chung 2006; Galve et al. 2009, 2011):

$$P = 1 - \{1 - p_{sc}\}^{\frac{n_s}{n_c}} \quad (2)$$

where:

- $p_{sc}$ is the proportion of pixels expected to be in motion in the next year in the susceptibility class, a parameter computed on the basis of the step decreasing monotonic function.
- $n_s$ is the number of pixels mobilized each year, that is, the mean frequency estimated from the multitemporal landslide inventory.
- $n_c$ is the number of pixels in the susceptibility class.

In practice, the steps to transform the susceptibility model into the hazard model were the following. First, the susceptibility model was reclassified into five classes according to the segments of an interval-defined non-increasing monotonic function fitted to the frequency of landslides in each of the original 200 susceptibility classes (see Fabbri et al. 2003 for further explanations). Second, Eq. 2 was applied to each of the five classes to estimate the annual probability of each pixel moving in the future.

It is worth noting that the meaning of our model is different from conventional landslide hazard models that contain the probability of a pixel being impacted by a landslide. According to the criteria behind our model, the value of each pixel indicates the probability of that pixel moving the following year. We take this probability value following the simplest interpretation of the frequentist probability. According to the frequentist interpretation, probability is understood as the frequency of an event repeated in a given time. If annual probability has a value of 1, it means the event will occur once a year. If its value is 0.1, the frequency is 1/10, hence the event is expected to occur at least once every 10 years, so that each year there is a 10% probability of occurence, or in other words, the event will happen in one of ten possible future years. In turn, by adding the values of the pixels covering a certain area, we can estimate the probability of that area being moved by a landslide. If the probability in a pixel is 0.1 and the class that contains that pixel has 10 pixels with that same value, we can expect that within the area covered by those pixels, at least one will move every year ($0.1 \times 10 = 1$). AQ3

# Results

## Inventory of landslides

A total of 292 landslides were inventoried dating from 1999 to 2015 (Fig. 3a), with a mobilized area of 417.9 hectares. The most characteristic landslides of the Loja valley have lengths ranging from 100 to 250 m and widths of between 60 and 150 m, but landslides up to 1,200 m long and 250 m wide have also been mapped. Most mobilized volumes of material were determined between 15,000 $m^3$ and 750,000 $m^3$, but in some cases they cover up to 2,000,000 $m^3$. These magnitudes are approximate because the real dimensions

and geometries are difficult to determine, showing fuzzy limits in many cases. Most landslides began as creeping processes and often evolved into earth flows or complex movements. The distribution of landslides according to their typology is 55.7% creep type, 38.8% flow type, 4.5% translational and 1% rotational. It is important to stress that the approach proposed was performed as a whole when applied to creep and flow typologies. This consideration is derived since the general inventory shows a large percentage of landslides related to the creep and flow typology (95%), which are generally compound processes starting as creep that later evolve into flows. Figure 3b and d represent the inventories of landslides corresponding to the periods of years between 1999 and 2003; from 2003 to 2010; and from 2010 to 2015, respectively (Fig. 4).

## Susceptibility models

Once the validation analysis of each conditioning factor had been carried out, nine factors were selected (Fig. 5) as they better predict the test according to AUPRC values equal to or greater than 0.59: faults, lithology, geomorphology, profile curvature, flat curvature, standard curvature, slope, land use and TPI. Accordingly, these conditioning factors will be used to generate the different susceptibility models by applying different scores to them for each method proposed in this research.

In order to estimate their predictive capacity, and by combining the nine conditioning factors selected (Fig. 5), ten susceptibility models resulted from applying the two methodologies described (Table 2). The best susceptibility model resulted from the combination of six conditioning factors (lithology, slope, geomorphology, faults, TPI, land use). Figure 6 presents the susceptibility maps created by means of LR (Fig. 6a) and "Matrix" (Fig. 6b).

The maps obtained were reclassified into five equal area classes so as to compare the models. Table 3 shows the amount of area in hectares and in percentage that corresponds to each class of susceptibility. As can be seen, the classes occupy similar percentages.

A comparison matrix served to correlate the landslides and the six conditioning factors used for the susceptibility model (Fig. 7). According to the lithology variable, most landslides are associated to sandstones with clay and conglomerate lens (32%), followed by conglomerates with silty-sandy matrix and clays (23%). These lithologies are associated to the Belen and San Cayetano Fms., already identified by Soto et al. (2017) as the geological units most prone to landslides due to the plastic clays content (see Sect. 2). The land use variable indicates that most occur in grasslands (64%) and among crops (15.8%). This result is also coherent with the field observations and general knowledge. In grasslands and crop land lack the tree root action against slope instabilities and usually these areas are selected because their clayed soils, mostly related to the clayed bedrock prone to landsliding. Furthermore, human activities that transform landscape changing slope geometries and drainage may favour landslide processes. The geomorphology factor indicates that the relief unit with the greatest presence of movilized area is the "dissected slope surface" (69.7%), then the "slope surface" and "slope front" (7.7% and 7.6%, respectively) as can be expected because landslide processes are mainly distributed in the slopes. The slope variable shows that the highest percentage of area affected by landslides is between 10° and 20° of slope, with 35%, followed by the slopes between 5° and 10° (25.1%), and the slopes between 20°and 30° (20.4%). Indeed, in this instance, the slope does not appear to provide substantial information regarding susceptibility, as evidenced by the similar percentages across each slope class, although the area of each class could also operate in the susceptibility classification providing critical data. Furthermore, it is noteworthy that the landslides occur at lower gradients in Loja. This may be related as mentioned above with the action of plastic clays in the studied phenomena. The "distance to the faults" factor indicates that most movilized area is in the range greater than 1,000 m (59.2%), but is also the range that occupies the largest area of land; the range of 400 to 1,000 m represents 26.3% of moved area, which indicates that theoretically this variable will not have a high predictive capability but some influence seems to have as was initially selected by its preliminary validation. The TPI variable indicates logically that the majority of movilized area is in the hillside class, 60.9%.

### Validation of the susceptibility models

Interestingly, when validation tests were performed on the prediction curves (PRCs) derived from the best susceptibility models, the tests established coincident values of 0.77 for both methods. It is important to note that the "Matrix" method better recognizes the areas of highest susceptibility, but it defines a wide area as low susceptibility, coinciding with mobilized terrain units. LR does not provide such good results in the high susceptibility zone, but it discriminates well between a safe zone and at zone of low susceptibility. The result of the validation curve of the LR & "Matrix" combined model (Fig. 8) shows that the prediction capacity improves substantially, giving a value of 0.8.

## Hazard model

A spatio-temporal analysis of landslide occurrence in the Loja basin (Table 4) was carried out to estimate the mean

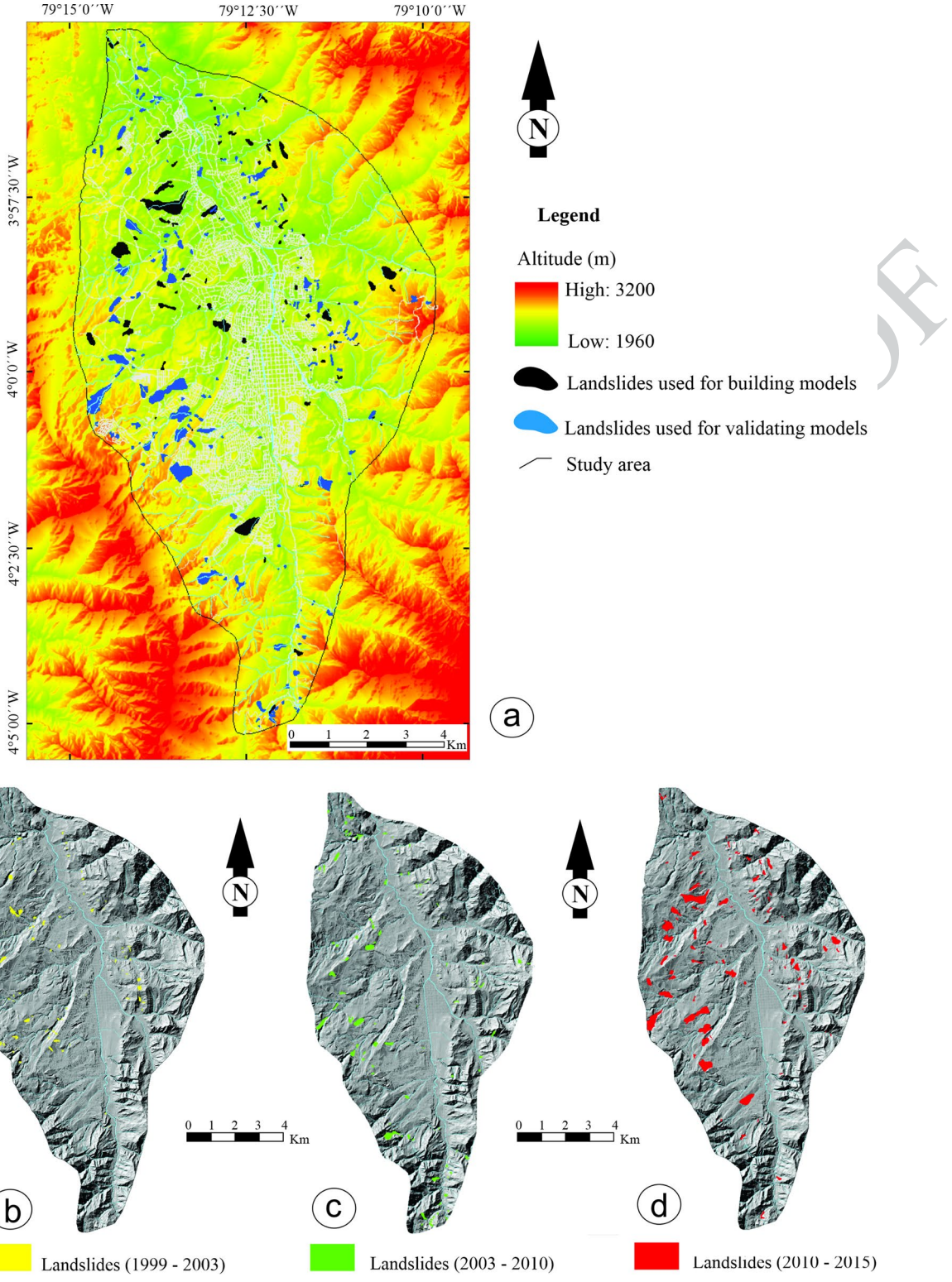


**Fig. 4** (**a**) Landslide inventory map, (**b-d**) multi-temporal inventory maps

annual frequency of pixels in motion to then produce the hazard model. We analyzed three different periods: P1 (1999–2003), P2 (2003–2010), P3 (2010–2015). We estimated that 31,604 pixels or 284,441 $m^2$ are mobilized by landslides per year in Loja on average. Relating the total of mobilized terrain pixels in the three periods (505,673) with the total number of landslides (310) corresponding to the three-time intervals, we obtained an average value of 1,631

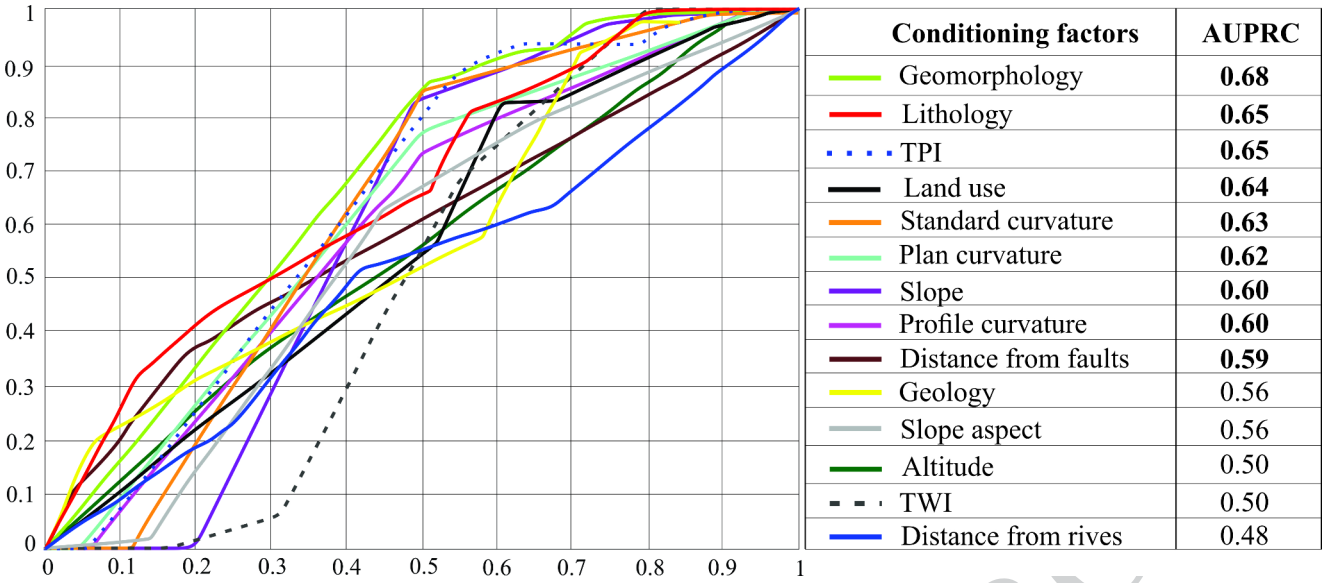


**Fig. 5** Diagrams of the validation curve of the 14 conditioning factors, using the Likelihood ratio, with their respective value of the area below the curve (AUPRC). Values highlighted in bold are those selected for the susceptibility models

**Table 2** AUPRC of the 10 susceptibility models generated with the Matrix method and likelihood ratio

| Conditioning factors | Matrix method | Likelihood ratio method |
|---|---|---|
| Distance to faults, lithology, slope degree, geomorphology, land use, TPI. | **0.77** | **0.77** |
| Distance to faults, lithology, geomorphology, land use, TPI. | 0.76 | 0.76 |
| Distance to faults, lithology, geomorphology, land use, distance to rivers. | 0.75 | 0.76 |
| Flat curvature, standard curvature, profile curvature, Distance to faults, lithology, slope degree, geomorphology, TPI. | 0.75 | 0.76 |
| Flat curvature, standard curvature, distance to faults, lithology, slope degree, geomorphology, TPI. | 0.75 | 0.76 |
| Standard curvature, distance to faults, lithology, slope degree, geomorphology, TPI | 0.75 | 0.76 |
| Distance from faults, lithology, slope, geomorphology, TPI | 0.75 | 0.76 |
| Distance to faults, lithology, geomorphology, TPI. | 0.74 | 0.75 |
| Lithology, geomorphology. | 0.67 | 0.71 |
| All factors. | 0.71 | 0.74 |

pixels or 14,680 $m^2$ per landslide. Finally, the ratio of mobilized ground pixels per year (31,604) to the mean value of movilized terrain pixels caused by landslides (1,631) indicates that 19 landslides occurred or are reactivated per year on average. Likewise, the distribution of landslide size in the study area was analysed (Table 5), based on the inventory.

Once the mean annual frequency of pixels in motion had been estimated, we used the the function fitting shown in Fig. 9 to apply Eq. 2 and generate the hazard model of Fig. 10.

Since the hazard map is completely quantitative, we can hardly make observations about the forecasting it performs or obtain useful information for risk management. The three most hazardous classes represent 38% of the study area (4,100 ha) (Table 6) where the majority (85%) of pixels that moved annually (34,494 pixels) are concentrated. In turn, there is a relatively safe area (very low hazard) that occupies 25% of the study area (2,698 ha) where the model predicts that only 1% of the pixels correspond to terrain prone to sliding (0.4 ha). Between these two large areas, there is a low-hazard class that extends across an area similar to the total area of the three most hazardous classes (37%). In this class, the model indicates that 14% (5 ha) of the pixels can move annually (Table 6).

With the above data in mind, and taking into account the distribution of landslide size (Table 5), we can estimate the annual number of landslides anticipated for each of the groups of classes. By dividing the pixels of the mobilized terrain units between different categories of landslide size, we can roughly estimate the number of landslides to be expected in the areas covered by each hazard class. Thus, in the area occupied by the three most hazardous classes

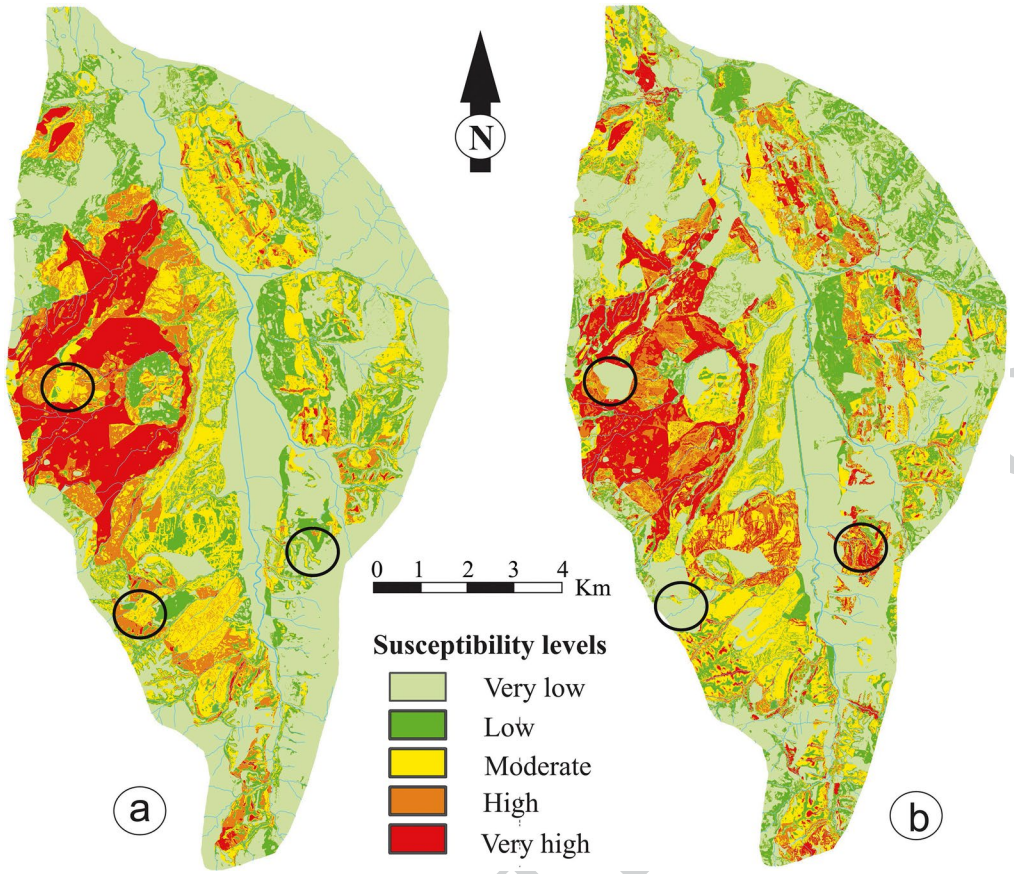


**Fig. 6** Landslide susceptibility map derived from the Likelihood ratio model (**a**) and Matrix model (**b**). The circles indicate the areas where the difference in the level of susceptibility generated between the two models is most evident

**Table 3** Comparison of the area occupied by each class of susceptibility generated by the two models

| Method | Susceptibility level | | | | | | | | | |
|---|---|---|---|---|---|---|---|---|---|---|
| | Very low | | Low | | Medium | | High | | Very high | |
| | ha | % | ha | % | ha | % | ha | % | ha | % |
| Matriz | 4,881.1 | 45.1 | 1,600.8 | 15 | 2,178.9 | 20.2 | 1,056.7 | 9.7 | 1,074.5 | 9.9 |
| LR | 4,866.1 | 45.2 | 1,620.1 | 14.8 | 2,185.2 | 20.2 | 1,048.1 | 9.8 | 1,072.6 | 10 |

(medium, high and very high), around 22 landslides a year might be triggered or reactivated; in the less hazardous zones (low and very low), the number of landslides expected would be around 4, most probably located in the low hazard zone (Table 7).

## Preliminary evaluation of the hazard model

At the beginning of 2018, a landslide inventory was carried out based on field work and the compilation of all information on landslides. A total of 45 new and reactivated landslides were registered during 2016 and 2017. Although a 2-year dataset is not statistically adequate for medium- to long-term predictions, it does permit a preliminary evaluation of the degree of fit of the hazard model. Due to the limited data, this evaluation was carried out by simplifying the model in the two groups of classes defined in the previous section. This model based on two groups accurately predicts the percentage of pixels corresponding to landsliding in each zone in 2016 and 2017 (Table 8), therefore forecasting the model that resembles what actually happened. If we go into depth and validate the five-classes model, we observe that the model deviates further into the medium hazard class, but the low and very low hazard classes define the affected area correctly (Table 8). Regarding the prediction of the number of landslides in each zone and their size, it is seen that the simple model based on two groups of classes predicts quite well the events registered during 2016 and 2017 (Table 9).

Because the model is designed to reflect an average of at least one to two decades, a larger registry would be needed to appraise the real forecasting capacity of the model. Still, we can affirm that the record of the two years following the

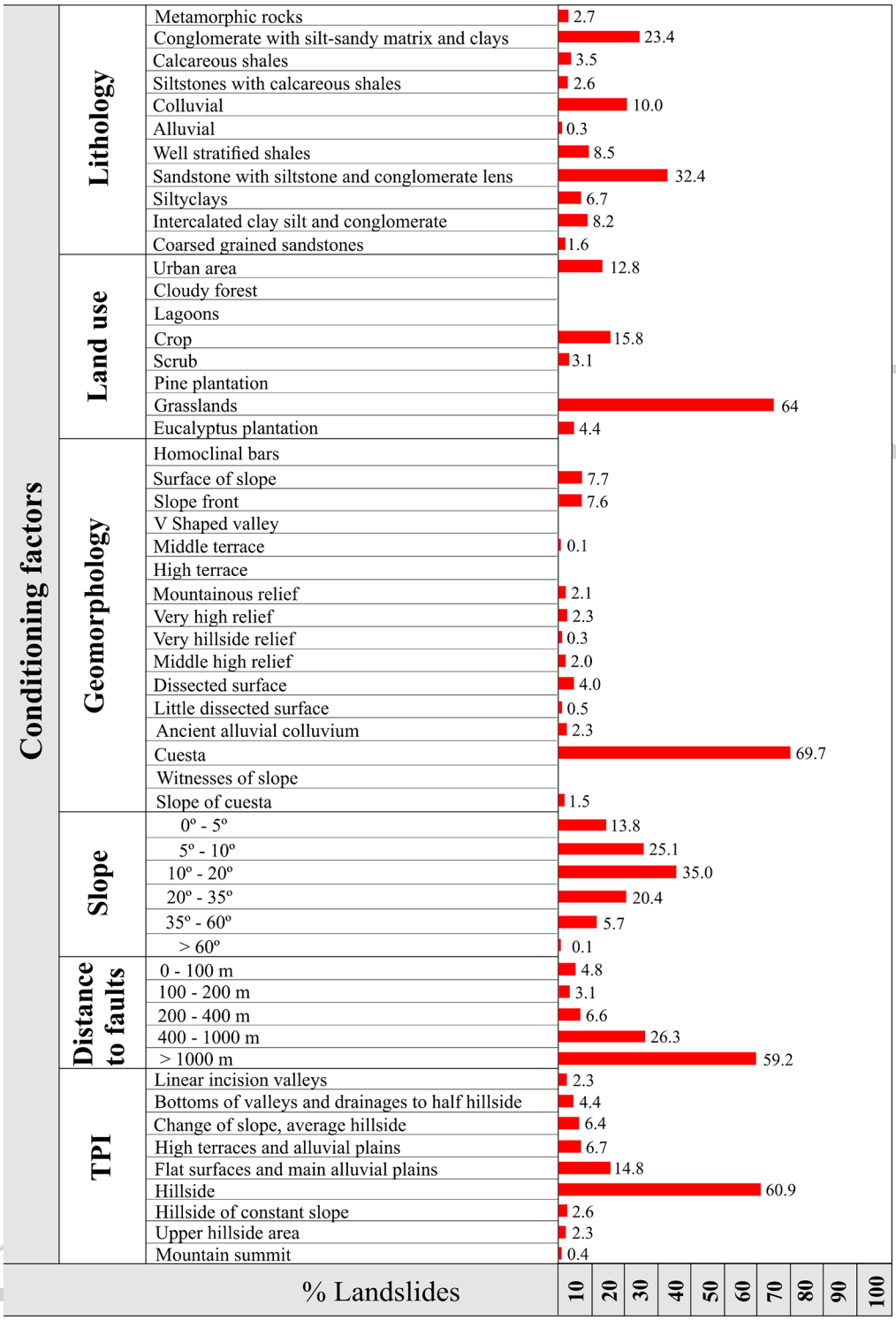


**Fig. 7** Comparison matrix between the conditioning factors selected for the analysis and their classes with the percentage of landslides

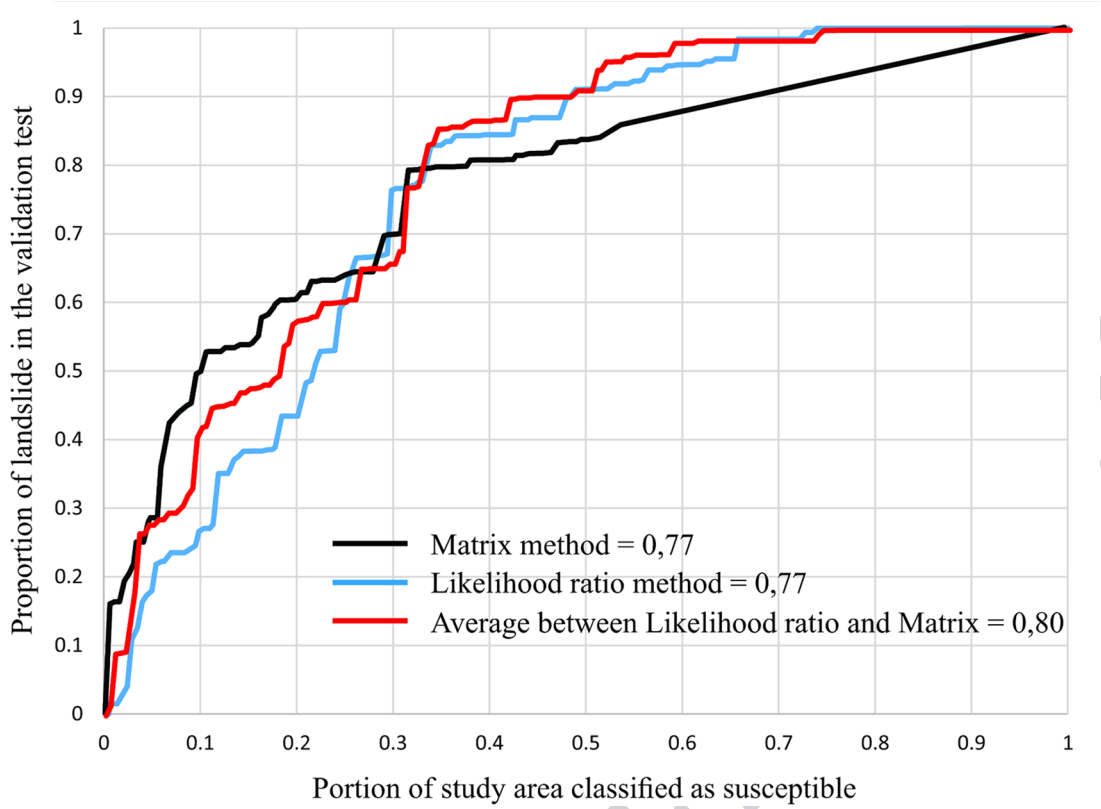


**Fig. 8** Representation of the validation curve of each of the applied methods, and additionally, the validation curve as a result of the average between the two methods

**Table 4** Spatio-temporal analysis of landslides, given inventories in the 3 periods considered

| Period | Landslides | Moving pixels | Years |
|---|---|---|---|
| P1 (1999–2003) | 84 | 58,813 | 4 |
| P2 (2003–2010) | 111 | 128,745 | 7 |
| P3 (2010–2015) | 115 | 318,114 | 5 |
| **Total** | **310** | **505,673** | 16 |

**Table 5** Distribution of sizes of landslides in the inventory

| Landslides size | Area (ha) | Average area (pixels) | Pixels per landslides size | % |
|---|---|---|---|---|
| Very Large | 25 – 15 | 23,486.3 | 7,268 | 21.1 |
| Large | 15 – 5 | 9,436.5 | 10,220 | 29.6 |
| Medium | 5-1.5 | 3,293.3 | 7,134 | 20.7 |
| Small | 1.5–0.5 | 974.6 | 7,615 | 22.1 |
| Very small | < 0.5 | 205.4 | 2,257 | 6.5 |

realization of the model fits the prediction reasonably well. In general, the data recorded lies in the same range, and in some cases perfectly matches the forecast.

## Discussion

Quantitative landslide hazard models are excellent tools for land planning in mountain areas. With them, spatial planners can calculate losses and check different alternatives for urban development or infrastructure projects. Yet it is very difficult to collect all the information needed to produce these models, for which reason they have only been made for certain places affording sufficient temporal and spatial data (e.g., Zêzere et al. 2004; Remondo et al. 2005; Nefeslioglu et al. 2011; Das et al. 2011; Jaiswal et al. 2011; Sanda et al. 2015; Galve et al. 2015, 2016). Here we present an area where a model was successfully produced, performing well despite being made with classical techniques.

We opted to focus our efforts on: (1) preparing a comprehensive database, taking into consideration all relevant details; (2) adopting a simple approach that combines all the information gathered; and (3) validating the model by means of a widely-accepted technique. The result is a model one can readily understand and its approximate performance

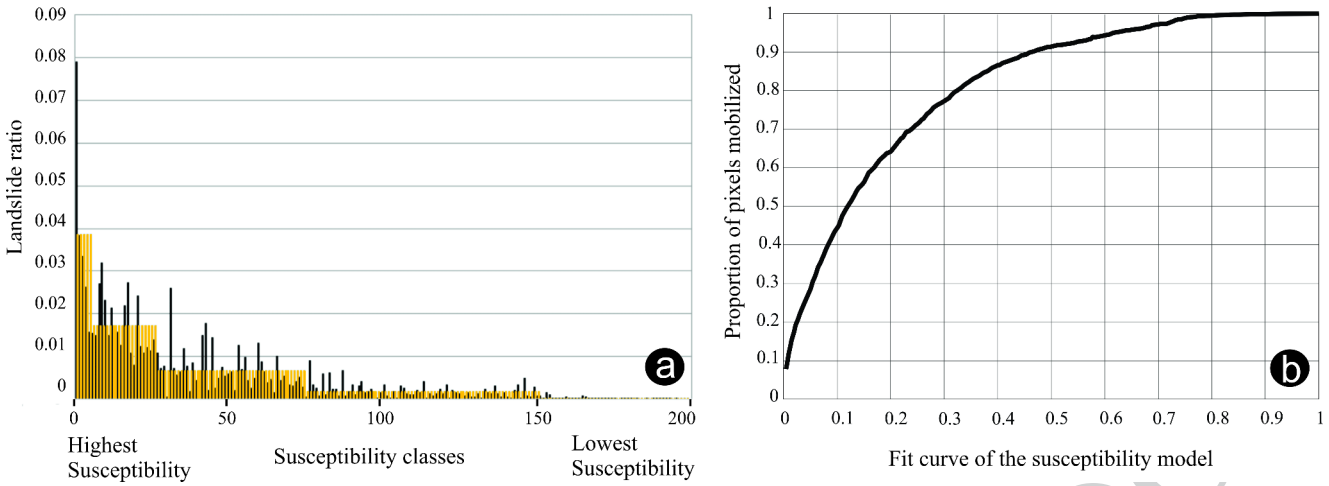


**Fig. 9** (**a**) Histogram of frequencies of landslides that occurred in each of the different susceptibility classes of the model, (**b**) Fit curve of the susceptibility model

is assessed through its validation. By "understanding the model" we refer to the fact that the resulting hazard pattern is evidenced in the spatial pattern of the conditioning factors, so that we know which factor(s) define high or low hazard in each area. This strength allows for extrapolation and improvement of our model, in light of local conditioning factors. Such problems or aspects can include: (1) misclassification of a geology unit or land-use class, (2) erroneous or deficent categoritation of a variable, and (3) defects in the elaboration of the conditioning factor maps. Once identified a problem, we can fix it. These methods moreover serve as a guide when focusing on the improvement of variables with a favourable balance between cost and benefit. Notwithstanding, methods applied with tools that come as default in extensively used GIS softwares (e.g., ArcGIS or QGIS), if they perform well, are widely applicable, since they require no specific training on advanced techniques or specialized software, nor (a priori) high computational performance.

It is also important to highlight that our model presents a distinct approach to landslide prediction. While the model estimates the probability of motion for specific portions of terrain—a common technique—we innovatively aggregate these results according to the observed landslide size distribution. This allows us to estimate how many landslides are expected to be reactivated or initiated in the future, categorized by their size (Tables 7 and 9). In other words, the model provides estimates that can indicate potential future reactivations of known large slow-moving earthflows, as well as the occurrence of new landslides, as demonstrated by the validation of the presented hazard model.

Thus, we adapted the hazard analysis to large slow-moving earthflows, a type of landslide that is widespread in clayey and marly terrains (Hungr et al. 2014). As these landslides also cause great economic losses in many regions in the world (Lacroix et al. 2020), the methodology applied here could serve to produce models intended to manage the risk associated with such slope movements.

On the downside, a deficiency detected in our model is that the influence of human activity may have been underestimated —the only variable that represents it is a static land-use map. Moreover, any other impact from human activity on producing this type of event cannot be ruled out. The demand for territory owing to urban and population expansion, implies constant activities such as: excavation, landfill, new residential development, opening of roads, forestry actions and agricultural activities, all entailing hydrological changes. Hence, such interventions can be seen as preparatory agents; that is, despite not being the direct cause of slope movements, in combination with other triggering agents they contribute to increasing the number of landslides. Future enhancements of the model should take into account all land use changes and the incorporation of data regarding local human activity.

To conclude this discussion, it is important to note that the developed landslide hazard model provides the Loja municipality with a tool precise enough to analyze landslide risk within its territory, as corroborated by its spatiotemporal validation. Current efforts are now focused on acquiring data regarding personal and economic losses to produce a risk model offering information in monetary or personal risk terms. With this information at hand, strategies to reduce or mitigate risks through spatial planning can be implemented objetively and optimized (e.g. Galve et al. 2012a, b). At the same time, models with greater forecast capacity using the lessons learning in the described process and using advanced methods based on AI will be developed to be applied in a subsequent risk analysis cycle.

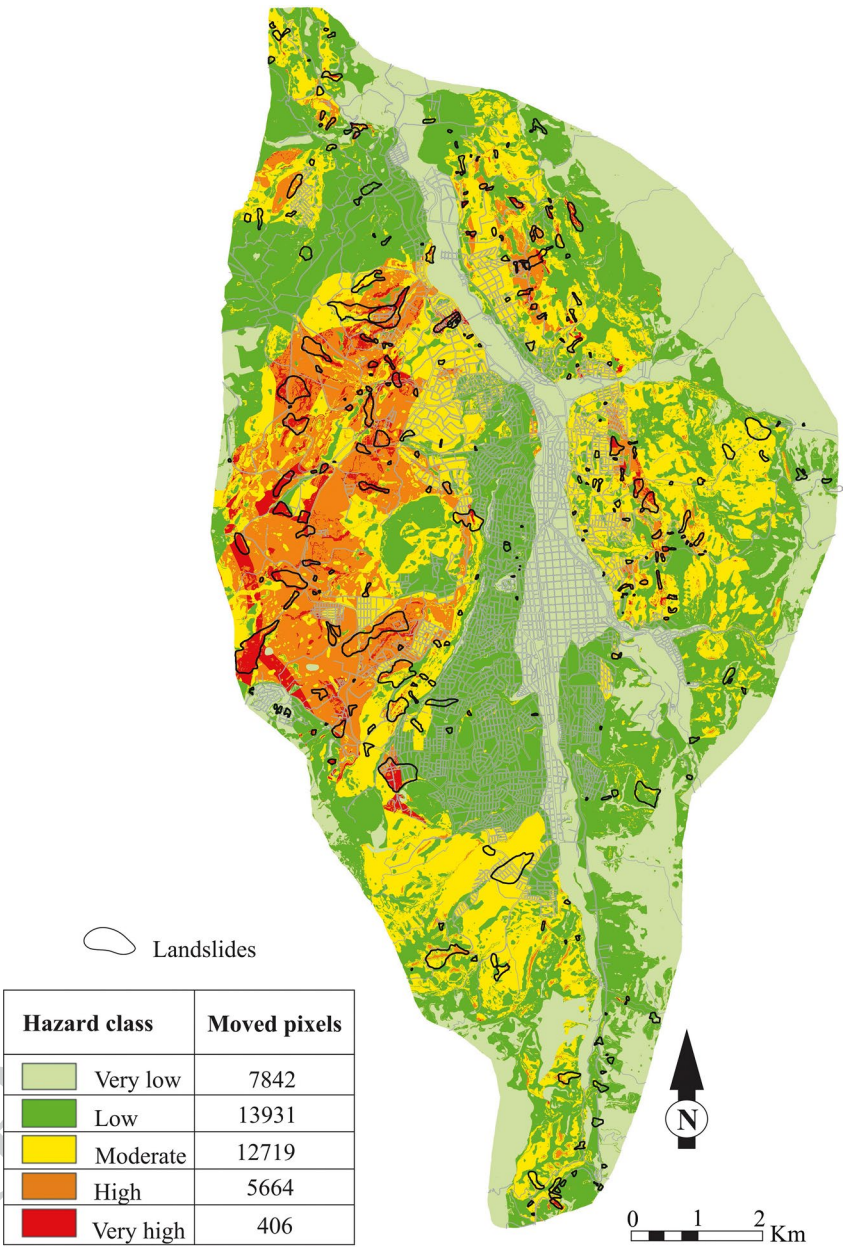


**Fig. 10** Hazard map of landslides with the location of inventoried landslides

**Table 6** Estimates of pixels moved annually by hazard class and hazard zones

| Hazard class | % of area per class | % of area per zone | Pixels moved per class | Píxeles moved per zone | % of pixels moved per class |
|---|---|---|---|---|---|
| Very high | 2 | 38 | 7,842.6 | 34,492 | 19.3 |
| High | 11 | | 13,931.6 | | 34.3 |
| Medium | 24 | | 12,719.9 | | 31.4 |
| Low | 37 | 62 | 5,664.2 | 6,070.5 | 14.0 |
| Very Low | 25 | | 406.2 | | 1.0 |

## Conclusions

In this study, we developed a robust quantitative landslide hazard model tailored for the Loja region in Ecuador. We applied a combination of two probabilistic methods to produce a landslide susceptibility model: the "Matrix" and the "Likelihood Ratio" methods. The models with highest predictive capability were achieved through the integration of six conditioning factors: distance to faults, lithology, slope, geomorphology, Topographic Position Index (TPI), and land use. While both methods demonstrated comparable performance, the "Matrix" method excelled in predicting

**Table 7** Estimates of the number of annual landslides by hazard class

| Size of landslides | Area (ha) | % | Medium to very high hazard | | Low to very low hazard | |
|---|---|---|---|---|---|---|
| | | | Pixels | Landslide per year | Pixels | Landslide per year |
| Very large | 25 – 15 | 21.1 | 7,268 | 0 | 1,279 | 0.1 |
| Large | 15 – 5 | 29.6 | 10,220 | 1 | 1,799 | 0.2 |
| Medium | 5-1.5 | 20.7 | 7,134 | 2 | 1,255 | 0.4 |
| Small | 1.5–0.5 | 22.1 | 7,615 | 8 | 1,340 | 1.4 |
| Very small | < 0.5 | 6.5 | 2,257 | 11 | 397 | 1.9 |
| | | | Total | 22 | | 3.9 |

**Table 8** Percentage of pixels anticipated to move and actually moved, by class

| Class | Hazard | Area | Model | Reality |
|---|---|---|---|---|
| Hazard model with 2 classes | | | | |
| 5-4-3 | High | 38% | 85% | 85% |
| 2 – 1 | Low | 62% | 15% | 15% |
| Hazard model with 5 classes | | | | |
| 5 | Very high | 2% | 19% | 12% |
| 4 | High | 11% | 34% | 31% |
| 3 | Medium | 24% | 31% | 43% |
| 2 | Low | 37% | 14% | 15% |
| 1 | Very low | 25% | 0% | 1% |

**Table 9** Number of landslides by size in each class of the model with two classes (two years)

| Size of landslides | Area | Zone of high hazard | | Zone of low hazard | |
|---|---|---|---|---|---|
| | | Hazard: Very high, high, medium | | Hazard: Low, very low | |
| | | Model | Inventored | Model | Inventored |
| Very large | 25 – 15 ha | 0 | 0 | 0 | 0 |
| Large | 15 – 5 ha | 2 | 0 | 0 | 0 |
| Medium | 5–1.5 ha | 4 | 4 | 0 | 0 |
| Small | 1.5–0.5 ha | 16 | 10 | 3 | 3 |
| Very small | < 0.5 ha | 22 | 27 | 4 | 7 |
| Total landslides | | 44 | 41 | 7 | 10 |

areas of high susceptibility, whereas the "Likelihood Ratio" method was more effective in identifying the safest zones. The synergy of these two approaches resulted in a mixed model with an AUPRC of 0.80, indicating strong spatial predictive capability.

The susceptibility model was subsequently transformed into a hazard model by integrating spatial predictions with the temporal frequency of landslides in the study area. This model allowed us to estimate potential future reactivations of existing landslides, as well as the occurrence of new ones. In other words, it enables us to predict future landslide activity in the municipality of Loja, including the number and size of landslides that may occur or reactivate annually. Based on the model, we estimate that 22 landslides per year will occur in Loja on average, primarily concentrated in the highest hazard zone which cover 38% of the study area. Of these landslides, three of them are expected to be larger than 1.5 hectares with a high damaging capacity. Additionally, the model delineates a low hazard area covering 62% of the study area, where only four small landslides (< 1.5 ha) are anticipated annually.

A preliminary validation of the hazard model, using landslide data from 2016 and 2017—collected after the model was developed—showed that the areas classified by the model according to their spatio-temporal probability aligned well with the frequency of landslides that occurred during these years. This alignment indicates that the methodologies employed and the variables selected contribute to a model that is both reliable and accurate.

The applied procedure and estimates are specifically tailored for large, slow-moving earthflows and have the potential to be applied in other regions of the Andean belt or globally, where similar landslide phenomena occur. Moreover, the methods used, which are based on accessible and easy-to-apply classical spatial analysis techniques, deliver effective and reliable results. In practice, these methods offer sufficient forecasting capability to support landslide hazard assessments and take initial steps in landslide risk management.

**Author contributions** J.S.L. and J.P.G. developed the analysis, wrote the main manuscript text and prepared figures and tables. J.A.P., J.M.A and C.I. concived the presented study, aided in interpreting the results

and reviewed the manuscript drafts. J.T. and G.G.J. helped in the field work, provided data and support technical tasks. All authors discussed the results and commented on the manuscript.

**Funding** This study was supported by the Secretaría de Educación Superior, Ciencia, Tecnología e Innovacion (SENESCYT) under the scholarship program "Open Call 2012 Second Phase" of the government of Ecuador and the Universidad Técnica Particular de Loja (Ecuador). The work of J.P.G. and J.M.A. was supported by the "Ramón y Cajal" Programme (RYC-2017-23335) of the Spanish Ministry of Science; the project "MORPHOMED" (PID2019-107138RB-I00) funded by MCIN / SRA (State Research Agency / https://doi.org/10.13039/501100011033); and FEDER/Junta de Andalucía-Consejería de Transformación Económica, Industria, Conocimiento y Universidades/Projects (B-RNM-305-UGR18, A-RNM-508-UGR20 and P18-RT-3632). Access to the Geohazard Exploitation Platform (GEP) of the European Space Agency (ESA) was provided by the NoR Projects Sponsorship (Project ID: 63737).

**Data availability** No datasets were generated or analysed during the current study.

## Declarations

**Competing interests** The authors declare no competing interests.

## References

Adedeji OH, Odufuwa BO, Adebayo OH (2012) Building capabilities for flood disaster and hazard preparedness and risk reduction in Nigeria: need for spatial planning and land management. J Sustainable Dev Afr 14(1):45–58

Alcántara-Ayala I, Oliver-Smith A (2014) ICL Latin-American Network: on the road to landslide reduction capacity building. Landslides 11(2):315–318

Aleotti P, Chowdhury R (1999) Landslide hazard assessment: summary review and new perspectives. Bull Eng Geol Environ 58(1):21–44

Arnould M, Frey P (1977) Analyse detaillée des réponses à l'enquête internationale sur les glissements de terrain. *Report to Unesco (with Summary in English)*

AQ4 Baeza C (1994) Evaluación de las condiciones de rotura y la movilidad de los deslizamientos superficiales mediante el uso de técnicas de análisis multivariante. PhD Thesis. Univ. Pol. Catalunya (Spain)

Baeza C, Corominas J (2001) Assessment of shallow landslide susceptibility by means of multivariate statistical techniques. Earth Surf Proc Land 26(12):1251–1263

Barella CF, Sobreira FG, Zêzere JL (2019) A comparative analysis of statistical landslide susceptibility mapping in the southeast region of Minas Gerais state, Brazil. Bull Eng Geol Environ 78:3205–3221

Bonachea J (2006) Desarrollo, aplicación y validación de procedimientos y modelos para la evaluación de amenazas, vulnerabilidad y riesgo debidos a procesos geomorfológicos. PhD Thesis. University of Cantabria (Spain)

Bonachea J, Remondo J, De Terán JRD, González-Díez A, Cendrero A (2009) Landslide risk models for decision making. Risk Anal 29(11):1629–1643

Boualla O, Mehdi K, Fadili A et al (2019) GIS-based landslide susceptibility mapping in the Safi region, West Morocco. Bull Eng Geol Environ 78:2009–2026

Bowman E (2015) Small landslides-frequent, costly, and manageable. In Landslides Hazards, Risks, and Disasters. Davies, T. (Ed.) Amnsterdam: Elsevier. https://doi.org/10.1016/B978-0-12-396452-6.00012-4

Bryan A (2016) Groundwater recharge of a landslide: an Isotopic and Meteorological Analysis. Univ Honors Theses Paper 311. https://doi.org/10.15760/honors.270 AQ5

Buolamwini J, Gebru T (2018) Gender Shades: Intersectional Accuracy Disparities in Commercial Gender Classification. In S. A. Friedler & C. Wilson (Eds.), Proceedings of the 1st Conference on Fairness, Accountability and Transparency (Vol. 81, pp. 77–91). PMLR AQ6

Cardinali M, Reichenbach P, Guzzetti F et al (2002) A geomorphological approach to the estimation of landslide hazards and risks in Umbria, Central Italy. Nat Hazards Earth Syst Sci 2:57–72

Chacón J, Irigaray C, Fernández T, El Hamdouni R (2006) Engineering geology maps: landslides and geographical information systems. Bull Eng Geol Environ 65(4):341–411

Chen W, Ding X, Zhao R, Shi S (2016a) Application of frequency ratio and weights of evidence models in landslide susceptibility mapping for the Shangzhou District of Shangluo City, China. Environ Earth Sci 75:64. https://doi.org/10.1007/s12665-015-4829-1

Chen W, Li W, Chai H, Hou E, Li X, Ding X (2016b) GIS-based landslide susceptibility mapping using analytical hierarchy process (AHP) and certainty factor (CF) models for the Baozhong region of Baoji City, China. Environ Earth Sci 75(1):63

Chung CJ (2006) Using likelihood ratio functions for modeling the conditional probability of occurrence of future landslides for risk assessment. Comput Geosci 32(8):1052–1068

Chung CJ, Fabbri AG (1993) The representation of geoscience information for data integration. Nat Resour Res 2(2):122–139

Chung CF, Fabbri AG (2005) Systematic procedures of landslide hazard mapping for risk assessment using spatial prediction models. *Landslide hazard and risk. Wiley, New York*, 139–177

Chung CJ, Fabbri AG (2008) Predicting landslides for risk analysis—spatial models tested by a cross-validation technique. Geomorphology 94(3):438–452

Chung CF, Frabbri AG (1999) Probabilistic prediction models for landslide hazard mapping. Photogram Eng Remote Sens 65(12):1389–1399 AQ7

Chung CF, Fabbri AG, Van Westen CJ (1995) Multivariate regression analysis for landslide hazard zonation. In: Carrara A, Guzzetti F (eds) Geographical information system in assessing natural hazards. Kluwer Academic, Dordrecht, pp 107–134 AQ8

Corominas J (1992) Landslide risk assessment and zoning. Plann Use Earth's Surf, 141–173

Dahal A, Tanyas H, van Westen C et al (2024) Space–time landslide hazard modeling via ensemble neural networks. Nat Hazards Earth Syst Sci 24:823–845

Das I, Stein A, Kerle N, Dadhwal VK (2011) Probabilistic landslide hazard assessment using homogeneous susceptible units (HSU) along a national highway corridor in the northern Himalayas, India. Landslides 8:293–308

DeGraff JV, Charles Romesburg H (1980) Regional Landslide Susceptibility Assessment for Wildland Management. A Matrix Approach

dos Santos Alvalá RC, de Assis Dias MC, Saito SM et al (2019) Mapping characteristics of at-risk population to disasters in the context of Brazilian early warning system. Int J Disaster Risk Reduct 41:101326

Einstein HH (1988) Special lecture: landslide risk assessment procedure. Proc 5th Int Symp Landslides Lausanne 2:1075–1090

Eras M (2014) Determinación de zonas susceptibles a movimientos en masa en el Ecuador, a escala 1:1.000.000 utilizando el método de ponderación de parámetros. Bsc Thesis. Escuela Politécnica Nacional (Ecuador)

Ercanoglu M, Gokceoglu C (2004) Use of fuzzy relations to produce landslide susceptibility map of a landslide prone area (West Black Sea Region, Turkey). Eng Geol 75(3–4):229–250
Fabbri A, Chung CJ, Cendrero A, Remondo J (2003) Is prediction of future landslides possible with a GIS. Nat Hazards 30(3):487–499
Fang Z, Wang Y, van Westen C, Lombardo L (2024) Landslide hazard spatiotemporal prediction based on data-driven models: estimating where, when and how large landslide may be. Int J Appl Earth Obs Geoinf 126:103631
Feizizadeh B, Blaschke T (2013) GIS-multicriteria decision analysis for landslide susceptibility mapping: comparing three methods for the Urmia lake basin. Iran Nat Hazards 65:2105–2128
Fell R, Corominas J, Bonnard C et al (2008) Guidelines for landslide susceptibility, hazard and risk zoning for land use planning. Eng Geol 102:85–98
Fernández T, El Hamdouni R, Irigaray C, Chacón J (2000) Metodología para la elaboración de cartografía de susceptibilidad a los movimientos de ladera, Colegio Oficial de Ingenierios Técnicos en Topografía, ed., *VII Congreso Nacional de Topografía y Cartografía*, TOP-CART 2000, Madrid, Spain, pp. 610–620
Galve JP, Gutiérrez F, Lucha P et al (2009) Probabilistic sinkhole modelling for hazard assessment. Earth Surf Processes Land 34:437–452
Galve JP, Remondo J, Gutiérrez F (2011) Improving sinkhole hazard models incorporating magnitude–frequency relationships and nearest neighbor analysis. Geomorphology 134:157–170
Galve JP, Gutiérrez F, Guerrero J, Alonso J, Diego I (2012a) Application of risk, cost–benefit and acceptability analyses to identify the most appropriate geosynthetic solution to mitigate sinkhole damage on roads. Eng Geol, 144–145, 65–77
Galve JP, Gutiérrez F, Guerrero J, Alonso J, Diego I (2012b) Optimizing the application of geosynthetics to roads in sinkhole-prone areas on the basis of hazard models and cost-benefit analyses. Geotext Geomembr 34:80–92
Galve JP, Cevasco A, Brandolini P, Soldati M (2015) Assessment of shallow landslide risk mitigation measures based on land use planning through probabilistic modelling. Landslides 12(1):101–114
Galve JP, Cevasco A, Brandolini P et al (2016) Cost-based analysis of mitigation measures for shallow-landslide risk reduction strategies. Eng Geol 213:142–157
Gantimurova S, Parshin A, Erofeev V (2021) GIS-Based landslide susceptibility mapping of the Circum-Baikal Railway in Russia using UAV Data. Remote Sens 13:3629
Gerzsenyi D, Albert G (2021) Landslide inventory validation and susceptibility mapping in the Gerecse Hills, Hungary. Geo Spat Inf Sci 24:498–508
González-Díez A (1995) Cartografía de movimientos de ladera y su aplicación al desarrollo temporal de los mismos y de la evolución del paisaje. Ph.D. Thesis. Univ. of Oviedo (Spain)
González-Díez A, Remondo J, de Terán JRD, Cendrero A (1999) A methodological approach for the analysis of the temporal occurrence and triggering factors of landslides. Geomorphology 30(1):95–113
Guzzetti F (2002) Landslide hazard assessment and risk evaluation: overview, limits and prospective. Proceedings 3rd MITCH Workshop Floods, Droughts and Landslides, pp. 24–26
Guzzetti F, Carrara A, Cardinali M, Reichenbach P (1999) Landslide hazard evaluation: a review of current techniques and their application in a multi-scale study, Central Italy. Geomorphology 31(1–4):181–216
Hamza T, Raghuvanshi TK (2017) GIS based landslide hazard evaluation and zonation–A case from Jeldu District, Central Ethiopia. J King Saud University-Science 29(2):151–165
Haque CE, Burton I (2005) Adaptation options strategies for hazards and vulnerability mitigation: an international perspective. Mitig Adapt Strat Glob Change 10(3):335–353
Hermanns RL, Valderrama P, Fauqué L, Penna IM, Sepúlveda S, Moreiras S, Zavala Carrión B (2012) Landslides in the Andes and the need to communicate on an interandean level on landslide mapping and research. Rev Asoc Geol Argent 69(3):321–327
Hungerbühler D, Steinmann M, Winkler W, Sewards D, Egüez A, Peterson DE, Helg U, Hammer C (2002) Neogene stratigraphy and Andean geodynamics of southern Ecuador. Earth Sci Rev 57:75–124
INEC (2010) Instituto Nacional de Estadísticas y Censos. VII Censo de población y VI de vivienda. Ecuador. http://www.inec.gob.ec
Irigaray C (1995) Movimientos de Ladera: Inventario, Análisis y Cartografía de la Susceptibilidad Mediante un Sistema de Información Geográfica. Aplicación a las Zonas de Colmenar (Málaga), Rute (Córdoba) y Montefrío (Granada). Unpublished PhD Thesis, Department of Civil Engineering, University of Granada, Spain, p. 578
Irigaray C, Lamas F, El Hamdouni R, Fernández T, Chacón J (2000) The importance of the precipitation and the susceptibility of the slopes for the triggering of landslides along the roads. Nat Hazards 21(1):65–81
Irigaray C, Fernández T, El Hamdouni R, Chacón J (2007) Evaluation and validation of landslide-susceptibility maps obtained by a GIS matrix method: examples from the Betic Cordillera (southern Spain). Nat Hazards 41(1):61–79
Jaiswal P, van Westen CJ, Jetten V (2011) Quantitative assessment of landslide hazard along transportation lines using historical records. Landslides 8(3):279–291
Kavoura K, Sabatakakis N (2020) Investigating landslide susceptibility procedures in Greece. Landslides 17:127–145
Lacasse S, Nadim F (2009) Landslide risk assessment and mitigation strategy. In: Sassa K, Canuti P (eds.) Landslides—disaster risk reduction. Springer, Berlin, Sect. 3, p 31–61. ISBN/ISSN: 978-3-540-69966-8. https://doi.org/10.1007/978-3-540-69970-5_3
Lacroix P, Handwerger AL, Bièvre G (2020) Life and death of slow-moving landslides. Nat Reviews Earth Environ 1(8):404–419
Lamb HH (1977) Climate history and the future. Methuen, London, p 212 AQ9
Larsen MC (2008) Rainfall-triggered landslides, anthropogenic hazards, and mitigation strategies. Adv Geophys 14:147–153
Lee S, Talib JA (2005) Probabilistic landslide susceptibility and factor effect analysis. Environ Geol 47(7):982–990
Li B, Liu K, Wang M et al (2022) Global Dynamic Rainfall-Induced Landslide susceptibility mapping using machine learning. Remote Sens 14:5795
Lima P, Steger S, Glade T, Murillo-García FG (2022) Literature review and bibliometric analysis on data-driven assessment of landslide susceptibility. J Mt Sci 19:1670–1698
Manchar N, Benabbas C, Hadji R et al (2018) Landslide Susceptibility Assessment in Constantine Region (NE Algeria) by means of statistical models. Studia Geotech et Mech 40:208–219
McBean GA, Henstra D (2003) Climate change, natural hazards and cities. Institute for Catastrophic Loss Reduction
Mondini AC, Guzzetti F, Melillo M (2023) Deep learning forecast of rainfall-induced shallow landslides. Nat Commun 14:2466
Moreno M, Lombardo L, Crespi A et al (2024) Space-time data-driven modeling of precipitation-induced shallow landslides in South Tyrol, Italy. Sci Total Environ 912:169166
Nefeslioglu HA, Gokceoglu C, Sonmez H, Gorum T (2011) Medium-scale hazard mapping for shallow landslide initiation: the Buyukkoy catchment area (Cayeli, Rize, Turkey). Landslides 8(4):459–483
Nocentini N, Rosi A, Piciullo L et al (2024) Regional-scale spatiotemporal landslide probability assessment through machine learning and potential applications for operational warning systems: a case study in Kvam (Norway). https://doi.org/10.1007/s10346-024-02287-9. Landslides

Nsengiyumva JB, Luo G, Amanambu AC et al (2019) Comparing probabilistic and statistical methods in landslide susceptibility modeling in Rwanda/Centre-Eastern Africa. Sci Total Environ 659:1457–1472

O'Hare GREG, Rivas S (2005) The landslide hazard and human vulnerability in La Paz City, Bolivia. Geographical J 171(3):239–258

Ozdemir A, Altural T (2013) A comparative study of frequency ratio, weights of evidence and logistic regression methods for landslide susceptibility mapping: Sultan mountains, SW Turkey. J Asian Earth Sci 64:180–197

Palamakumbure D, Flentje P, Stirling D (2015) Consideration of optimal pixel resolution in deriving landslide susceptibility zoning within the Sydney Basin, New South Wales, Australia. Comput Geosci 82:13–22

Palenzuela JA, Jiménez-Perálvarez JD, Chacón J, Irigaray C (2016a) Assessing critical rainfall thresholds for landslide triggering by generating additional information from a reduced database: an approach with examples from the Betic Cordillera (Spain). Nat Hazards 84(1):185–212

Palenzuela JA, Jiménez-Perálvarez JD, El Hamdouni R et al (2016b) Integration of LiDAR data for the assessment of activity in diachronic landslides: a case study in the Betic Cordillera (Spain). Landslides 13:629–642

Persichillo MG, Bordoni M, Meisina C, Bartelletti C, Barsanti M, Giannecchini R, D'AmatoAvanzi G, Galanti Y, Cevasco A, Brandolini P, Galve JP (2017) Shallow landslidessusceptibility assessment in different environments. Geomatics Nat Hazards Risk 8(2):748–771

Petley D (2012) Global patterns of loss of life from landslides. Geology 40:927–930

Petley D, Dunning SA, Rosser NJ (2005) The analysis of global landslide risk through the creation of a database of worldwide landslide fatalities. Landslide risk management. Balkema, Amsterdam, pp 367–374

PNUMA MDLNCI (2007) Perspectivas del Medio Ambiente Urbano: GEO Loja

Pollock W (2020) A framework for regional scale quantitative landslide risk analysis. University of Washington

Pourghasemi HR, Pradhan B, Gokceoglu C (2012) Application of fuzzy logic and analytical hierarchy process (AHP) to landslide susceptibility mapping at Haraz watershed, Iran. Nat Hazards 63(2):965–996

Raghuvanshi TK, Negassa L, Kala PM (2015) GIS based Grid overlay method versus modeling approach–A comparative study for landslide hazard zonation (LHZ) in Meta Robi District of West Showa Zone in Ethiopia. Egypt J Remote Sens Space Sci 18(2):235–250

Reichenbach P, Rossi M, Malamud BD, Mihir M, Guzzetti F (2018) A review of statistically-based landslide susceptibility models. Earth Sci Rev 180:60–91

Remondo J (2001) Elaboración y validación de mapas de susceptibilidad de deslizamientos mediante técnicas de análisis especial, Ph.D. thesis, Universidad de Oviedo, Spain

Remondo J, González-Díez A, De Terán JRD, Cendrero A (2003) Landslide susceptibility models utilising spatial data analysis techniques. A case study from the lower Deba Valley, Guipúzcoa (Spain). Nat Hazards 30(3):267–279

Remondo J, Bonachea J, Cendrero A (2005) A statistical approach to landslide risk modelling at basin scale: from landslide susceptibility to quantitative risk assessment. Landslides 2(4):321–328

Sahrane R, El Kharim Y, Bounab A (2022) Investigating the effects of landscape characteristics on landslide susceptibility and frequency-area distributions: the case of Taounate province, Northern Morocco. Geocarto Int 1–27

Sanda R, Ştefan B, Dănuţ P et al (2015) Application of landslide hazard scenarios at annual scale in the Niraj River basin (Transylvania Depression, Romania). Nat Hazards 77:1573–1592

Schuster RL (1996) Socioeconomic effects of landslides, in Turner, A. K., Transportation Research Board Special Report 247 AQ10

Schuster RL, Krizek R (1978) Landslides: analysis and control. Unknown

Seibert J, Stendahl J, Sorensen R (2007) Topographical influences on soil properties in borealforests. Geoderma 141:139–148

Shano L, Raghuvanshi TK, Meten M (2020) Landslide susceptibility evaluation and hazard zonation techniques – a review. https://doi.org/10.1186/s40677-020-00152-0. Geoenvironmental Disasters 7. AQ11

SIGTIERRAS (2010) Ortofotografía Escala 1:5000 Generada a. Partir de la Toma de Fotografía Aérea

SNGR/ECHO/UNISDR (2012) Secretaría Nacional De Gestión De Riesgos. Referencias Básicas para la Gestión de Riesgos. Quito, Ecuador, Ecuador

Soeters R, van Westen CJ (1996) Landslides: Investigation and mitigation. Chapter 8-Slope instability recognition, analysis, and zonation. *Transportation research board special report* (247)

Soto J (2018) Análisis de la peligrosidad frente a los movimientos de ladera en la cuenca de Loja (Ecuador). University of Granada (Spain). PhD Thesis. https://digibug.ugr.es/bitstream/handle/10481/51128/2907101x.pdf

Soto J, Galve JP, Palenzuela JA, Azañón JM, Tamay J, Irigaray C (2017) A multi-method approach for the characterization of landslides in an intramontane basin in the Andes (Loja, Ecuador). Landslides 14(6):1929–1919

Soto J, Palenzuela JA, Galve JP, Luque JA, Azañón JM, Tamay J, Irigaray C (2019) Estimation of empirical rainfall thresholds for landslide triggering using partial duration series and their relation with climatic cycles. An application in southern Ecuador. Bull Eng Geol Environ 78(3):1971–1987

Stanley TA, Kirschbaum DB, Benz G et al (2021) Data-Driven Landslide Nowcasting at the global scale. Front Earth Sci Chin 9. https://doi.org/10.3389/feart.2021.640043

Tamay J (2018) Estructura de cuencas intramontañosas del sur de Ecuador en relación con la tectónica de la Cordillera de los Andes a partir de datos geofísicos y geológicos. University of Granada (Spain). PhD Thesis. https://digibug.ugr.es/bitstream/handle/10481/51634/29096297.pdf

Tamay J, Galindo-Zaldívar J, Ruano P, Soto J, Lamas F, Azañón JM (2016) New insight on the recent tectonic evolution and uplift of the southern Ecuadorian Andes from gravity and structural analysis of the Neogene-Quaternary intramontane basins. J S Am Earth Sci 70:340–352

UNESCO (1973–1979) Annual summaries of information on natural disasters, 1971–1975. UNESCO, Paris

Van Phong T, Phan TT, Prakash I et al (2021) Landslide susceptibility modeling using different artificial intelligence methods: a case study at Muong Lay district, Vietnam. Geocarto Int 36:1685–1708

van Westen CJ, Castellanos E, Kuriakose SL (2008) Spatial data for landslide susceptibility, hazard, and vulnerability assessment: an overview. Eng Geol 102:112–131

Wieczorek G, Glade T (2005) Climatic factors influencing occurrence of debris flows. In: Jakob M, Hungr O (eds) Debris-flow hazards and related phenomena. Springer, Berlin, pp 325–362. https://doi.org/10.1007/3-540-27129-5_14.

Zêzere JL, Reis E, Garcia R, Oliveira S, Rodrigues ML, Vieira G, Ferreira AB (2004) Integration of spatial and temporal data for the definition of different landslide hazard scenarios in the area north of Lisbon (Portugal). Nat Hazards Earth Syst Sci 4(1):133–146

| | |
|---|---|
| Journal: | **12665** |
| Article: | **11905** |

**AQ1.** Please specify clearly which reference should be linked whether (Palenzuela et al. 2016a or 2016b) in all instances.

**AQ2.** References (Cueva 2015, Palenzuela 2015, Girma et al. 2015, Corominas et al. 2003, Fell et al. 2005, Corominas and Moya 2008, Corominas et al. 2014, Remondo 2003, Chung and Fabbri 1999, Carrara et al. 2008, Chen et al. 2018, Van Westen 2016, Highland and Bobrowsky 2008, Chung and Fabbri 1995, Chung and Fabbri 2003, Van Steijn 1991, Cendrero et al. 1994, Hungr et al. 2014) are cited in the text but not provided in the reference list. Please provide the respective references in the list or delete these citations.

**AQ3.** Please check and confirm if the inserted citation of Figure 4 is correct. If not please suggest an alternate citation.

**AQ4.** Citation for Reference (Baeza 1994) missing in the manuscript. Please check.

**AQ5.** Citation for Reference (Bryan 2016) missing in the manuscript. Please check.

**AQ6.** Citation for Reference (Buolamwini & Gebru 2018) missing in the manuscript. Please check.

**AQ7.** Citation for Reference (Chung & Frabbri 1999) missing in the manuscript. Please check.

**AQ8.** Citation for Reference (Chung et al. 1995) missing in the manuscript. Please check.

**AQ9.** Citation for Reference (Lamb 1977) missing in the manuscript. Please check.

**AQ10.** Citation for Reference (Schuster 1996) missing in the manuscript. Please check.

**AQ11.** Citation for Reference (Shano et al. 2020) missing in the manuscript. Please check.